universe

IMPACT FACTOR 2.813

CITESCORE 3.2

Article

Realization of Bounce in a Modified Gravity Framework and Information Theoretic Approach to the Bouncing Point

Sanghati Saha and Surajit Chattopadhyay

Topic Collection

Modified Theories of Gravity and Cosmological Applications

Edited by

Prof. Dr. Panayiotis Stavrinos and Prof. Dr. Emmanuel N. Saridakis

MDPI

https://doi.org/10.3390/universe9030136

universe

MDPI

Article

Realization of Bounce in a Modified Gravity Framework and Information Theoretic Approach to the Bouncing Point

Sanghati Saha and Surajit Chattopadhyay *

Department of Mathematics, Amity University Kolkata, Major Arterial Road, Action Area II, Newtown, Rajarhat, Kolkata 700135, India

* Correspondence: schattopadhyay1@kol.amity.edu or surajitchatto@outlook.com; Tel.: +91-9830736116 or +91-8240384649

Abstract: In this work, we report a study on bouncing cosmology with modified generalized Chaplygin Gas (mgCG) in a bulk viscosity framework. Reconstruction schemes were demonstrated in Einstein and modified $f(T)$ gravity framework under the purview of viscous cosmological settings. We also took non-viscous cases into account. We studied the equation of state (EoS) parameter under various circumstances and judged the stability of the models through the sign of the squared speed of sound. We observed the mgCG behaving like avoidance of Big Rip in the presence of bulk viscosity at the turnaround point and in non-viscous cases, a phantom-like behavior appears. The turnaround point equation of state parameter crosses the phantom boundary, violating NEC. The role of the mgCG's model parameters was also investigated before and after the bounce. A Hubble flow dynamics was carried out and, it was revealed that mgCG is capable of realizing an inflationary phase as well as an exit from inflation. An $f(T)$ gravitational paradigm was also considered, where the mgCG density was reconstructed in the presence of bulk viscosity. The role of the parameters associated with the bouncing scale factor, describing how fast the bounce takes place, was also studied in this framework. Finally, the reconstructed mgCG turned out to be stable against small perturbations irrespective of the presence of bulk viscosity and modified gravity scenario. Finally, the reconstruction scheme was assessed using statistical analysis, Shannon entropy.

Keywords: modified generelized Chaplygin gas; bulk viscosity; bounce scale factor; Einstein gravity; modified $f(T)$ gravity; null energy condition; Big Rip singularity; Shannon entropy

Citation: Sanghati, S.; Chattopadhyay, S. Realization of Bounce in a Modified Gravity Framework and Information Theoretic Approach to the Bouncing Point. *Universe* **2023**, *9*, 136. https://doi.org/10.3390/universe9030136

Academic Editors: Panayiotis Stavrinos and Yi-Fu Cai

Received: 9 January 2023
Revised: 22 February 2023
Accepted: 27 February 2023
Published: 6 March 2023

1. Introduction

Countless observational studies of the cosmic universe, viz. Ia Supernovae (SNe Ia) [1–4], the Cosmic Microwave Background (CMB) [5,6], Wilkinson Microwave Anisotropy Probe(WMAP) [7–11], large scale redshift surveys structure (LSS) [12–17], show that the current universe is in a phase of accelerated expansion [18]. Dark energy (DE) is the term given to a hypothetical fluid with negative pressure that is spearheading the universe's accelerating expansion. This gravitationally repulsive exotic energy exerts a repulsion characterized by the equation of state (EoS) parameter $w = \frac{p}{\rho} < -1/3$. Almost three fourths of total mass-energy density of the universe [19] is made up of this unknown cosmic fluid. Like dark matter, it is invisible. It can be detected from astrophysical observations between cosmic entities. Dark energy still remains an unknown form of energy. DE, the exotic energy, is in the stress–energy–momentum tensor of the field equations in Einstein's theory of general relativity. There is a direct correlation between the matter–energy of the universe and the global or local geometry of the universe in the General Theory of Relativity (GTR) [20–24]. DE is detected by its impact on the rate at which the universe expands and its effect on the rate at which galaxies and gravitationally bound groups of galaxies form through gravitational perturbations. The oldest explanation of dark energy is that it is an innate, fundamental energy density inherent to vacuum energy,

which is the key ingredient in Einstein's cosmological constant [25]. In [26], the method of regularization of vacuum energy is observed. Martin et al. briefly described the method of measurement of the cosmological constant as being constrained by experiments with planet orbits in our solar system or atomic spectra in cosmology. In [27], the global nature of the cosmological constant problem is emphasized by highlighting the significance of radiative instability as well as Weinberg's no-go theorem. In this lecture series, the defined sequester is a new representational approach to the cosmological constant problem that incorporates both general relativity and renormalization by cancellation of the standard model vacuum energy.

The simplest candidate of DE is Einstein's cosmological term symbolized as Λ with $\omega_\Lambda = -1$ [28–31], introduced by Albert Einstein to augment his field equations of the General Theory of Relativity. Numerous dark energy models having a time varying EoS parameter supported by observations such as quintessence [32–34], phantom [35–38], quintom [39–42], tachyon field [43–45], hessence [46–49], k-essence [50,51], Chaplygin gas [52–55], holographic dark energy [56–60], etc., have been presented to find out the cause behind the cosmic accelerated expansion. A broader picture of the various facets of DE review is available in the studies [61–70]. Cold dark matter (CDM) [71,72] is another dark component of the universe that presents $\Omega\sim0.3$ and is driven by the cosmological interpretation of the rotation curves of galaxies and the formation of a large-scale structure. Of late, a theoretical model has been proposed with the introduction of an unusual, hypothetical fluid, viz. Chaplygin Gas (CG) [73–75]. Chaplygin Gas is one of the many candidates for dark energy and it is capable of unifying CDM and DE. This is also a perfect fluid used in general relativity to model idealized distributions of matter, specified with the equation of state

$$p = -\frac{A}{\rho^\alpha}. \tag{1}$$

In this equation, p denotes pressure, density is denoted by ρ and A is a positive constant. Initially, it was proposed that $\alpha = 1$ [76]. Following that, according to the general conclusion, it was proposed that $\alpha \neq 1$ [77]. This equation of state, introduced by Sergey Chaplygin, serves as an effective mathematical approximation for calculating the aerodynamical lifting force on an aircraft wing. This isentropic fluid only admits a supersymmetric generalization. Chaplygin Gas plays an important role in telling the story of string theory. The foremost major feature of Chaplygin Gas is that it can describe a shift to the current stage of cosmic acceleration from a decelerated cosmic expansion and as a single substance, it can unify dark matter and dark energy, which together constitute the dark sector of the universe. This non-homogeneous Chaplygin Gas provides a broad realistic explanation uniting the disparate roles of DE and DM. This exotic fluid presents the simplest deformations of the most typical ΛCDM models. A. Kamenshchik and M. C. Bento proposed the generalized Chaplygin Gas (CGC) model [78,79] at the start of the 21st century, with $A > 0$ and $0 \leqslant \alpha \leqslant 1$ with equation of state Equation (1). Chaplygin Gas can easily interpolate between a non-relativistic matter phase of vanishing pressure $(p = 0)$ and a negative-pressure era dominated by DE [80]. A modified Chaplygin Gas (mCG) model was proposed by Debnath et al. [81] where isotropous pressure p of the cosmological fluid adheres to

$$p = A\rho - \frac{B}{\rho^\alpha}, \tag{2}$$

and $0 \leqslant A \leqslant 1, 0 \leqslant \alpha \leqslant 1$ and B is a positive constant. Fundamental characteristics of mCG as a DE candidate were studied in [82–84]. Because the behavior of CG is similar to that of dark matter (DM) with vanishing pressure in the early stages of the universe and similar to that of a cosmological constant in later phases, this significant and interesting behavior of the CG model has been widely studied in the literature [85]. Moreover, this model was expanded to several forms [86–88]. These developments were the prime motivation behind our study of the modified generalized Chaplygin Gas (mgCG) model along with the equation of state

$$p = \epsilon\rho - (1+\epsilon)A\rho^{-\gamma}, \tag{3}$$

where ϵ, A and γ are three real parameters.

Based on observational studies, we can say that our current universe is facing an accelerated expansion and it is important to note that this late-time acceleration is by no means the lone accelerated phase of the cosmos. In the preliminary stage, the inflationary phase is another phase of such expansion. Several irregularities of the Big Bang cosmology were accordingly communicated in the works of [89,90] within the framework of the inflationary cosmology exemplary for the early universe. Unification of early inflation and late-time cosmic acceleration was demonstrated in [91,92] and denoted a phantom cosmology uncovering the shift to the inflationary era, bearing in mind the transition to the non-phantom standard cosmology and retrieving the recently observed dark energy era. Furthermore, modern cosmologists continue to debate whether the universe began to expand as a result of a Big Bang singularity or as a result of a non-singular, bouncing scenario. Inflation is one of many cosmological scenarios that provides an explanation for the early universe and finds a possible answer to the horizon and flatness problems. In addition, it predicts an almost scale-invariant curvature perturbation power spectrum. However, tracing back in time, the inflationary scenario explains the consequences of an initial cosmic singularity, well known as the Big Bang singularity, where geodesic incompleteness causes the space-time curvature to diverge at the point of the space-time singularity.

A bouncing cosmology is an alternative to inflation that can produce a curvature power spectrum that is scale invariant and the bouncing scenario leads to non-singular universe evolution [92–102]. In the scenario of matter bouncing, the universe experiences a matter-dominated period with the onset of the contraction. In addition, a bounce occurs without any singularity. To put it another way, it implies that the universe transitioned from an accelerated collapse era to an expanding era over the bounce without exhibiting any singular behavior. Following the bounce, the universe immediately enters a phase of matter-dominated expansion. Beside the Big Bang singularity, there are many other types of finite-time singularities in cosmology studied in [103]. The severest amongst them is the Big Rip or Type-I singularity; however, there are another three similar finite time singularities, namely Type-II, Type-III or Type-IV singularities [104–108]. In the case of Type-I, II or III singularities, the universe's effective energy density and/or effective pressure diverge at the point of singularity. In contrast, in the Type-IV singularity, the effective energy density and the effective pressure of the universe stay finite during the instance of the singularity and consequently the Type-IV singularity is the milder one among the finite-time singularities. Specifically, unlike the Big Rip singularity, the geodesic incompleteness is absent in the Type-IV singularity. As a result, the universe can easily pass through a Type-IV singularity (if such a singularity exists) and the Type-IV has no catastrophic effects on observable quantities. Thus, it is possible that the universe encountered a Type-IV singularity in the past in the course of its evolution. It sailed through it without any geodesic incompleteness. Nevertheless, the existence of a Type-IV singularity might exercise noteworthy influence on the evolution of the universe, and also on the generation era of the primordial perturbation modes, as the singularity can globally influence the Hubble parameter.

Viscous cosmology plays a pivotal role within the scientific community in the evolution of the universe. A few studies and reviews on viscous cosmological analysis are presented in [109–114]. In this context, bulk viscosity is attributed to space isotropy and shear viscosity is linked to space anisotropy. Shear viscosities are not considered because the CMB describes meaningful anisotropies, so bulk viscosity can make a case for the universe's accelerated cosmic expansion. In the early universe, when studying inflationary cosmology, the concept of bulk viscosity was proposed in the literature without any requirement of dark energy. Hence, bulk viscosity could be one of the reasons for the current accelerated expansion of the universe. Nowadays, several authors have tried to explain the late-time acceleration via bulk viscosity without any dark energy constituent. In theory, deviations from local thermodynamic stability can cause bulk viscosity to form, but a detailed mechanism for bulk viscosity formation is still elusive. In cosmology, when the matter content of the

universe expands or contracts too fast as a cosmological fluid, then the effective pressure is generated to bring the system back to its thermal stability. The manifestation of such an effective pressure is bulk viscosity. To analyze the late acceleration of the universe, the casual theory, according to which viscosity propagates at a finite speed, has been used. Cataldo et al. [115] proposed a study on late-time acceleration using the casual theory of bulk viscosity. Basically, they used an ansatz for the Hubble parameter (inspired by the Eckart theory) and they have shown the transition of the universe from the Big Rip singularity to the phantom behavior.

In the expansion history of the universe, unifying early-phase inflation and later-phase acceleration can be felt in scalar-tensor gravity. Modified gravity provides a true union of early-time inflation and late-time acceleration in this case. It can also form the basis for explanations of both dark energy and dark matter [116,117]. Inflationary expansion of the universe has been observed in several modified gravity frameworks viz. $f(R)$ gravity [118], scalar curvature corrections to general relativity [119], higher-derivative quantum gravity [120], unimodular $f(T)$ gravity [121], mimetic $f(R)$ gravity [122,123] and $f(R,\phi)$ gravity [124]. An extension of the General Theory of Relativity is that modified gravity causes a transition from deceleration to acceleration in the evolution of the universe. By introducing a scalar field after the conformal transformation, we can use $f(R)$-modified gravity. Without choosing a DE candidate, $f(T)$ gravity, the other modified gravity with torsion T, can explain the late-time acceleration with the thermal expanding history of the universe [125–129]. Torsion's role in gravity has been extensively studied in recent decades, with the main goal of bringing gravity closer to its gauge formulation and incorporating spin in a geometric description. Based on the paradigm of $f(T)$ gravity, where $f(T)$ is an arbitrary function of the torsion scalar, we can incorporate cosmological and astrophysical applications both at the background and perturbation levels, in different eras along the cosmic expansion. The $f(T)$ gravity construction, as an alternative to a cosmological constant, can provide a theoretical interpretation of the late-time universe acceleration and it can easily accommodate the regular thermal expanding history, including the radiation and cold dark matter dominated phases. Furthermore, in the early universe, inflation could be achieved through the $f(T)$ paradigm and the Big Bang singularity could be avoided due to the appearance of non-singular bounces.

In information theory, the uncertainty of a random variable is called the entropy inherent to the variable's possible outcomes. The distribution of a discrete random variable X that accepts values from the alphabet $\mathcal{X}$ is as follows:

$$p : \mathcal{X} \to [0,1], \tag{4}$$

$$H(X) = -\sum_{i=1}^{n} P(x_i) \log P(x_i), \tag{5}$$

where Σ denotes the sum over possible values of the variable. Claude Shannon introduced the concept of information entropy in his 1948 paper "A Mathematical Theory of Communication" and that is why it is also referred to as Shannon entropy [130–135]. Shannon entropy is a measure of uncertainty in statistical thermodynamics theory. In probabilistic information theory, entropy is a measure of data produced uncertainty for some event or variable. The higher value of Shannon entropy reflects the higher level of uncertainty measured in the model. This evaluation is carried out on the basis of maximum entropy. There are several ways in which uncertainty can be found. However, the sources of uncertainty at the bouncing point have not been examined. In this study, we use the probabilistic information theory and the initial conditions to quantify uncertainty. Moreover, we incorporated sources of deterministic uncertainty in this model. Here, we considered two scenarios described as "pre" and "post" bounce scenarios. As this particular non-singular bouncing model favours a late-time cosmic speed-up phenomenon, we wanted to find the change in uncertainty for this speed-up. In this study, it is observed that the uncertainty is significantly higher near the bouncing point due to inflation.

The purpose of the present work is to have an insight into the bouncing behavior of mgCG under the purview of modified theory of gravity. Furthermore, another focus of the study is to implement a probabilistic information theory-based approach to discern how the models behave from the point of view of uncertainty theory. The evolution of uncertainty with changes in the mathematical expectations of the associated random variables is quantified through Shannon entropy, which is optimized by using the Lagrangian optimization method. Details are given in subsequent sections.The plan of the work is the following. In Section 2, we construct the mgCG realization of the bouncing scenario, drawing forth the corresponding analytical solutions. In Sections 3–8, we proceed to the reconstruction of generalized scenarios to explain inflationary expansion of the universe. Finally, Section 9 is devoted to finding the uncertainty towards the turnaround point and Section 10 is devoted to the conclusions.

2. Equation of State of Barotropic Fluid

Considering the bouncing scale factor [136] form of

$$a(t) = a_0\left(1 + \frac{3t^2\sigma}{2}\right)^{\frac{1}{3}}. \tag{6}$$

In this case, the scale factor at the turnaround point is a_0 and a positive parameter σ describes the bounce speed. Additionally, we have shown the advantages of taking semi-analytic solutions and this estimation of mathematical solutions demonstrates the existence of bouncing solutions in the framework of matter-dominated contraction and expansion. Therefore, from Equation (6), the derived Hubble parameter is

$$H = \frac{t\sigma}{1 + \frac{3t^2\sigma}{2}}. \tag{7}$$

Here, we have taken the background evolution fluid as barotropic mgCG whose equation of state (EoS) [137] is

$$p = \epsilon\rho - (1+\epsilon)A\rho^{-\gamma}, \tag{8}$$

where we have denoted thermodynamic pressure as p, total energy density as ρ and ϵ, A and γ parameterize Equation (8). The constraints on the mgCG barotropic fluid described above are $\epsilon > \frac{1}{3}$, $A > 0$ and $\gamma > 0$. The transition of the vanishing pressure phase can describe the evolution of the universe from a relativistic particle-dominated era ($\epsilon = \frac{1}{3}$) to a dark energy-dominated negative pressure era. Here, we considered the universe to be filled with dark energy and dark matter as a single component and neglected the contribution of other components throughout this paper whereas dark matter with no pressure results in $p_m = 0$. Therefore,

$$\rho = \rho_x + \rho_m, \tag{9}$$

where ρ_x denotes dark energy density, ρ_m denotes dark matter density and ρ denotes total energy density.

In a Friedmann–Robertson–Walker (FRW) universe dominated with bulk viscous fluid, the Friedmann field equations [138] are

$$\frac{6\ddot{a}}{a} = -(\rho + 3(p + \Pi)), \tag{10}$$

and

$$3H^2 = \rho_x + \rho_m, \tag{11}$$

where the universe's total energy density, originating from a scalar field of the background effective fluid is ρ. Here, we assumed that the background fluid is a viscous Chaplygin Gas that drives the early period of the universe's expansion, where Π is the bulk viscous

pressure and Π is described by $\Pi = -3H\xi$, where ξ is the viscosity coefficient, which is a function of the Hubble parameter. Again, from the conservation equation of pressureless dark matter, we know that

$$\dot{\rho_m} + 3H\rho_m = 0. \tag{12}$$

$$Or\ \rho_m = \rho_{m0}a(t)^{-3}. \tag{13}$$

From Equations (11) and (13), we obtain

$$\rho_x = 3H^2 - \rho_{m0}a(t)^{-3}. \tag{14}$$

From Equations (8) and (14) we obtain the expression of reconstructed p of mgCG.

$$p = -12^{-\gamma}A(1+\epsilon)\left(\frac{t^2\sigma^2}{(2+3t^2\sigma)^2}\right)^{-\gamma} + \frac{12t^2\epsilon\sigma^2}{(2+3t^2\sigma)^2}. \tag{15}$$

Therefore, the EoS parameter defined by $\omega = \frac{p}{\rho}$, where p is thermodynamic pressure and ρ is total energy density, can be derived from the form

$$\omega = \epsilon - 12^{-1-\gamma}A(1+\epsilon)\left(\frac{t^2\sigma^2}{(2+3t^2\sigma)^2}\right)^{-1-\gamma}. \tag{16}$$

Alternatively, ω can be written as

$$\omega = \epsilon - 12^{-1-\gamma}A(1+\epsilon)\left(\frac{(2+3t^2\sigma)^2}{t^2\sigma^2}\right)^{1+\gamma}. \tag{17}$$

In Equation (17), we can notice, at the bouncing point $t = 0$, the denominator becomes zero. The reconstructed density and EoS parameters are plotted in Figure 1 and Figure 2, respectively. The reason for this divergence in Figure 2 is as follows; in Equation (17), ϵ is a positive quantity and the following term tends to infinity towards the turnaround point for all parameter values.

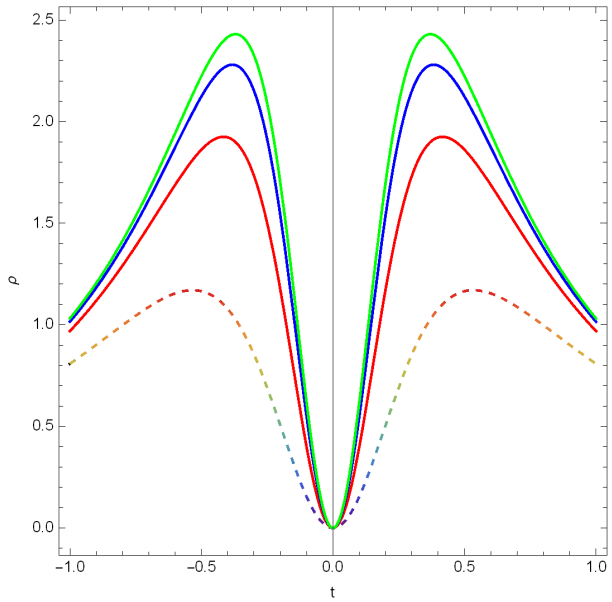

Figure 1. Reconstructed density evolution in the modified generalized Chaplygin Gas scenario with $\rho_{m_0} = 0.32$, $a_0 = 0.2$, $\epsilon = 0.43$, $\gamma = 0.89$ and $A = 0.96$ varying $\sigma = (2.34, 3.85, 4.56, 4.86)$ in units for rainbow-dashed, red-solid curve, blue-solid curve and green-solid curve, respectively, with the bouncing point arising at $t = 0$.

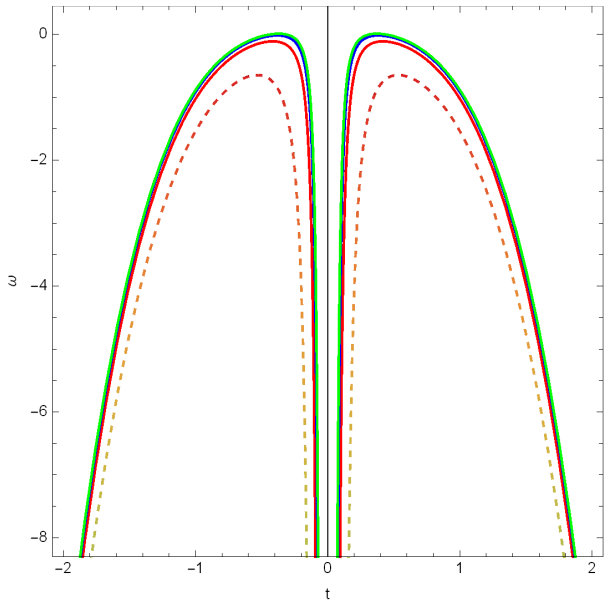

Figure 2. Reconstructed EoS parameter evolution in the modified generalized Chaplygin Gas scenario with $\rho_{m_0} = 0.32$, $a_0 = 0.2$, $\epsilon = 0.43$, $\gamma = 0.89$ and $A = 0.96$ varying $\sigma = (2.34, 3.85, 4.56, 4.86)$ in units for rainbow-dashed, red-solid curve, blue-solid curve and green-solid curve, respectively, with the bouncing point arising at $t = 0$.

From Equations (15) and (10), we obtained the expression of bulk viscous pressure (Π),

$$\Pi = \frac{12^{-\gamma}\left(\frac{t^2\sigma^2}{(2+3t^2\sigma)^2}\right)^{1-\gamma}\left(A(1+\epsilon)\left(2+3t^2\sigma\right)^2 - 3^\gamma 4^{1+\gamma}\sigma\left(\frac{t^2\sigma^2}{(2+3t^2\sigma)^2}\right)^\gamma\left(2+3t^2\epsilon\sigma\right)\right)}{t^2\sigma^2}. \tag{18}$$

By simplifying Equation (18), we can see that the denominator is zero at the bouncing point $t = 0$. For that reason, the evolution of the reconstructed bulk viscous pressure diverges in Figure 3 and increases infinitely towards the turnaround point.

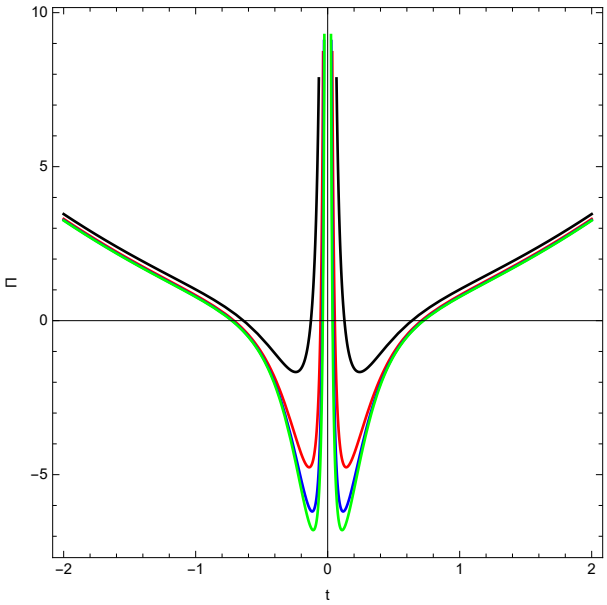

Figure 3. Reconstructed bulk viscous pressure Π evolution in the modified generalized Chaplygin Gas scenario with $\rho_{m_0} = 0.32$, $a_0 = 0.2$, $\epsilon = 0.43$, $\gamma = 0.89$ and $A = 0.96$ varying $\sigma = (2.34, 3.85, 4.56, 4.86)$ in units for black-solid, red-solid curve, blue-solid curve and green-solid curve, respectively.

Here, the bulk viscous pressure (Π) can be written as a function of Hubble parameter $\Pi = -3H\xi$ where ξ is the coefficient of viscosity. Then, reconstructed ξ can be written as:

$$\xi(H) = -\frac{3^{-1-\gamma}4^{-\gamma}\left(1+\frac{3t^2\sigma}{2}\right)\left(\frac{t^2\sigma^2}{(2+3t^2\sigma)^2}\right)^{1-\gamma}\left(A(1+\epsilon)\left(2+3t^2\sigma\right)^2-3^{\gamma}4^{1+\gamma}\sigma\left(\frac{t^2\sigma^2}{(2+3t^2\sigma)^2}\right)^{\gamma}\left(2+3t^2\epsilon\sigma\right)\right)}{t^3\sigma^3}. \tag{19}$$

Equation (19) can be simplified and towards bouncing point $t = 0$ the denominator tends to zero and that is why the evolution of the reconstructed viscosity coefficient diverges in Figure 4. The effective EoS parameter ω_{eff} can be defined as the ratio of effective pressure $(p + \Pi)$ and total energy density ρ. We can derive the expression of the effective EoS parameter from Equations (14), (15) and (18) which is plotted in Figure 5 with respect to cosmic time t. As bulk viscous pressure itself diverges towards the bouncing point, the effective EoS parameter also diverges.

We plotted the reconstructed mgCG density evolution with respect to cosmic time t in Figure 1 and discovered that mgCG energy density decreases due to contraction in the pre-bounce scenario, is the lowest at the bouncing point at $t = 0$ and increases after bounce due to expansion. This figure supports the inflationary expansion of the universe, as it depicts a rapid increase in density due to inflation, followed by density stabilization in later phases of the universe. The behavior of the background evolution of energy density in Figure 1 is continuous and well behaved. The bounce is clearly visible in Figure 2, the EoS parameter crosses the phantom boundary and there is an avoidance of Big Rip singularity in a viscous mgCG scenario in Figure 5. In Figures 3 and 4, we plotted bulk viscous pressure versus cosmic time t and viscosity coefficient ξ using $\Pi = -3H\xi$.

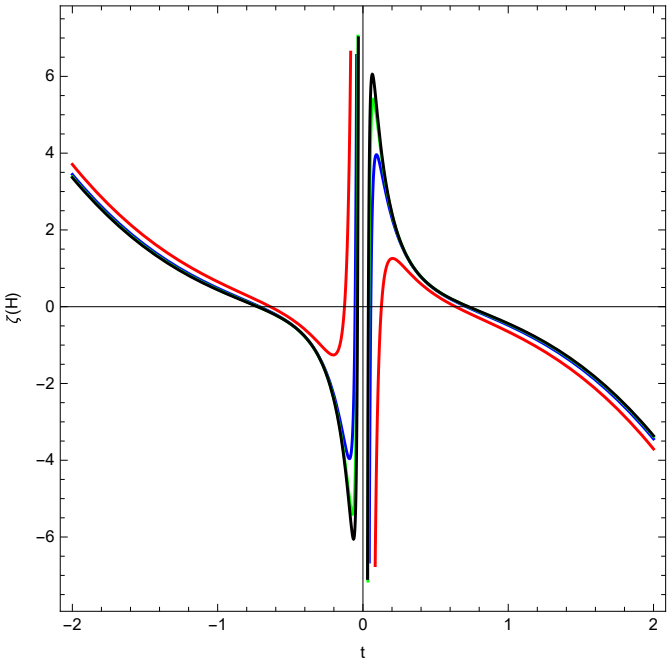

Figure 4. Reconstructed bulk viscosity coefficient ξ evolution in the modified generalized Chaplygin Gas scenario with $\rho_{m_0} = 0.32$, $a_0 = 0.2$, $\epsilon = 0.43$, $\gamma = 0.89$ and $A = 0.96$ varying $\sigma = (2.34, 3.85, 4.56, 4.86)$ in units for black-solid, red-solid curve, blue-solid curve and green-solid curve, respectively.

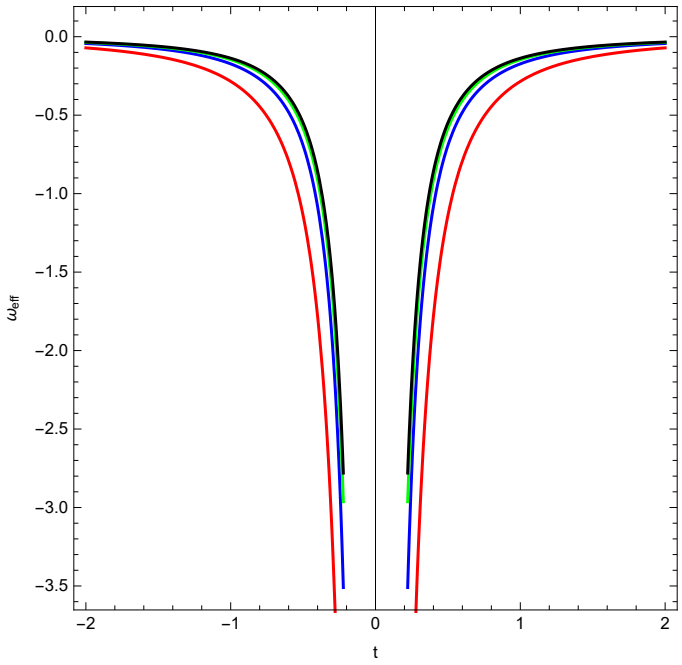

Figure 5. Reconstructed effective EoS parameter evolution in the modified generalized Chaplygin Gas scenario with $\rho_{m_0} = 0.32$, $a_0 = 0.2$, $\epsilon = 0.43$, $\gamma = 0.89$ and $A = 0.96$ varying $\sigma = (2.34, 3.85, 4.56, 4.86)$ in units for black-solid, red-solid curve, blue-solid curve and green-solid curve, respectively, with the bouncing point arising at $t = 0$.

3. Bounce Cosmology with Respect to E-Folding Number

We have demonstrated the theory of perturbations for the framework of mgCG evolution in every single bouncing layout associated with inflationary observables, which is important for us. In particular, the Hubble horizon decays faster than the wavelengths of the generated vacuum state fluctuations and contraction continues before the phase of bounce. The fluctuations after leaving the Hubble radius form bounce and later in the expanding phase, the fluctuations re-enter the inner parts of the horizon. Here, Equation (6) is the form of the bouncing scale factor where a_0 is the scale factor at the bouncing point and the positive parameter σ denotes the speed of the bounce. Therefore, Equation (7) is the derived Hubble parameter. Now, we considered the e-folding time scale N [139] in spite of cosmic time t, associated with the scale factor as shown:

$$e^{-N} = \frac{a_0}{a}. \tag{20}$$

Or $N = \ln(\frac{a}{a_0})$, which implies $H = \dot{N}$.
Therefore,

$$N = \frac{1}{3}\ln\left(1 + \frac{3t^2\sigma}{2}\right). \tag{21}$$

Then, we converted the cosmic time (t) in terms of e-folding number N and found the thermodynamic pressure p, density ρ and EoS parameter (ω) in terms of e-folding time scale.

$$t(N) = \pm\sqrt{\frac{2(-1+e^{3N})}{3\sigma}}. \tag{22}$$

and we obtained

$$p = 2e^{-6N}\left(-1+e^{3N}\right)\epsilon\sigma - 2^{-\gamma}A(1+\epsilon)\left(e^{-6N}\left(-1+e^{3N}\right)\sigma\right)^{-\gamma}. \tag{23}$$

$$\rho_{Total} = 2e^{-6N}\left(-1+e^{3N}\right)\sigma. \tag{24}$$

We have shown the evolution of the time derivative of e-fold number $\dot{N}$ versus time t in Figure 6. It has been demonstrated that the scale factor at the bouncing point, i.e., $a = a_0$; we have $N = 0$. In Figure 6, $\dot{N}$ is symmetric about the bouncing time $t = 0$ and it supports the realization of nonsingular bounce. It has been observed that before the bounce $t < 0$, we have $\dot{N} < 0$ due to contraction of the universe as $\dot{a} < 0$ and after the bounce $t > 0$, expanding attribute of $\dot{N}$ occurred due to expansion of the universe.

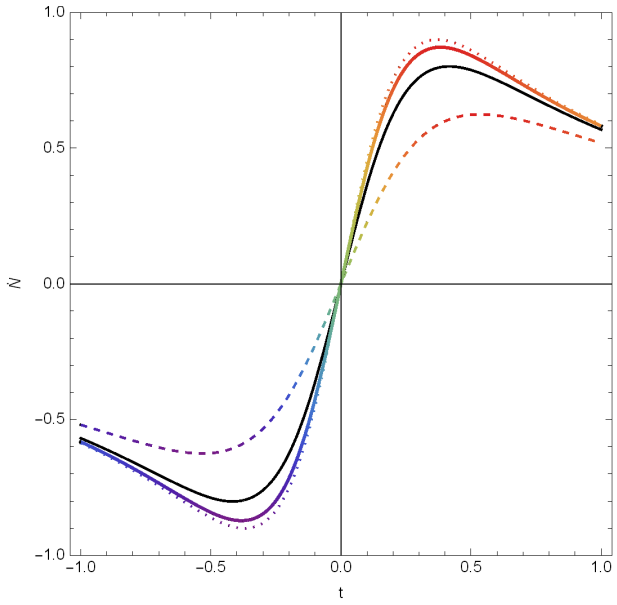

Figure 6. Evolution of expression of time derivative of e-folding Number with respect to cosmic time with $\rho_{m_0} = 0.32$, $a_0 = 0.2$, $\epsilon = 0.43$, $\gamma = 0.89$ and $A = 0.96$ varying $\sigma = (2.34, 3.85, 4.56, 4.86)$ in units for rainbow-dashed curve, rainbow-dotted curve, black-solid curve and rainbow-solid curve, respectively, the bouncing point at $t = 0$.

Here, we plotted the evolution of the expression of ω defined by $\omega = \frac{p}{\rho}$ and ω_{eff} defined by $\omega_{eff} = \frac{p+\Pi}{\rho}$ with respect to time derivative of the e-folding number in Figures 7 and 8.

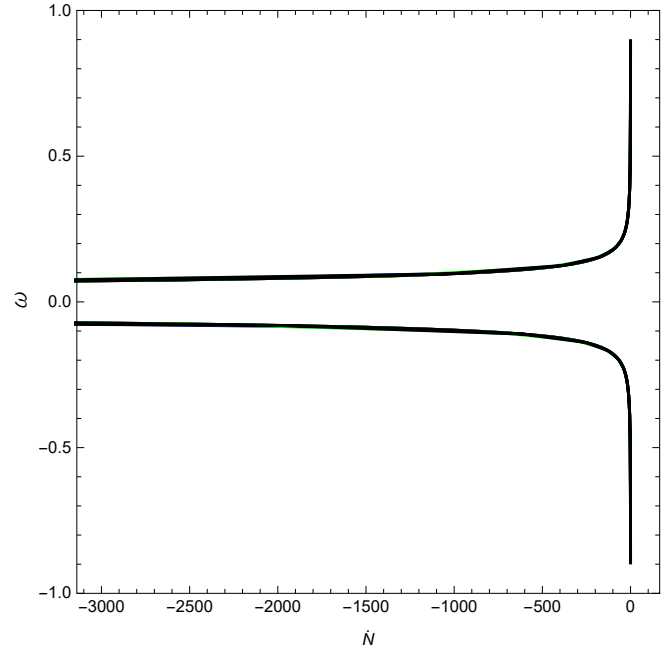

Figure 7. Evolution of expression of ω with respect to time derivative of e-folding number.

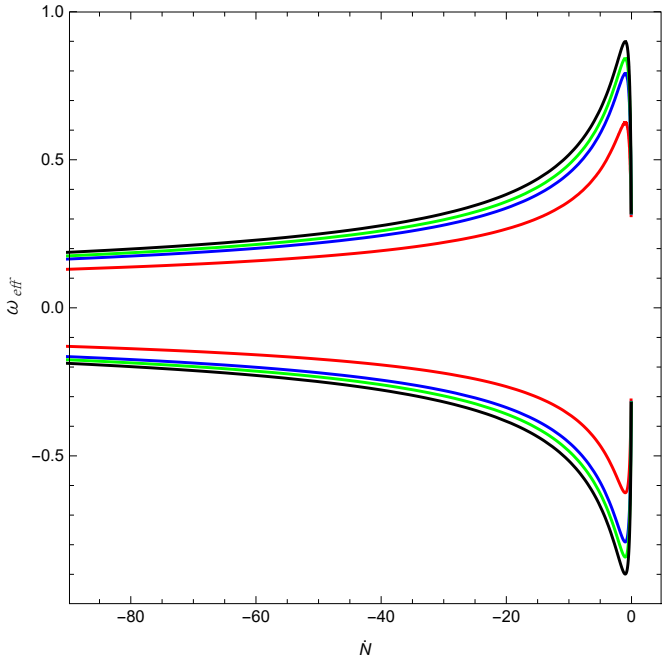

Figure 8. Evolution of expression of ω_{eff} with respect to time derivative of e-folding number.

4. Hubble Flow Dynamics

In the early universe, cosmic inflation is one of the main paradigms for explaining cosmological parameters and contains phase of exponential expansion of the universe and it accomplishes the paths for initiating in homogeneities on cosmological scales. We consider the Hubble flow parameters [140], proposed in the studies of cosmologists Hoffman [141], Turner [142] and Kinney, defined by

$$\epsilon_{i+1} = \frac{dln\epsilon_i}{dN}. \tag{25}$$

where N is the e-folding time scale.

$$\epsilon_1 = 1 - \frac{\ddot{a}}{aH^2} = -\frac{\dot{H}}{H^2}. \tag{26}$$

$$\epsilon_2 = \frac{\dot{\epsilon_1}}{H\epsilon_1}. \tag{27}$$

For inflation, $\ddot{a} > 0$, ϵ_1 has to be less than 1. It is very obvious for vanishing inflationary epoch ϵ_1 has to take the value of unity.

$$\epsilon_1 = \frac{3}{2} - \frac{1}{t^2\sigma}. \tag{28}$$

$$\epsilon_2 = \frac{-2}{t^2\sigma} + \frac{12}{-2+3t^2\sigma}. \tag{29}$$

Here, we plotted Hubble flow parameters in Figure 9 and Figure 10, respectively. From Figure 9 we can see at first ϵ_1 is symmetric about the turnaround point. It shows an increasing pattern before the bounce. Then, after the bounce it has an increasing pattern also. Hence, we understand that across the bounce $\epsilon_1 << 1$ that suits the required condition for inflation. After that, it crosses the boundary of $\epsilon_1 = 1$ and it indicates a nice exit from inflation. Thus, we have demonstrated the capability of realization of the inflationary era and as well as an exit from inflation with mgCG background fluid by Figure 10. In the pre-bounce scenario $H < 0$ and ϵ_1 and $\dot{\epsilon_1} < 0$. We have observed in Figure 10 just before bounce $\epsilon_2 < 0$ which supports the theory and immediately after the bounce $H > 0$ and ϵ_2 is also less than zero by supporting inflation. Then, it becomes positive.

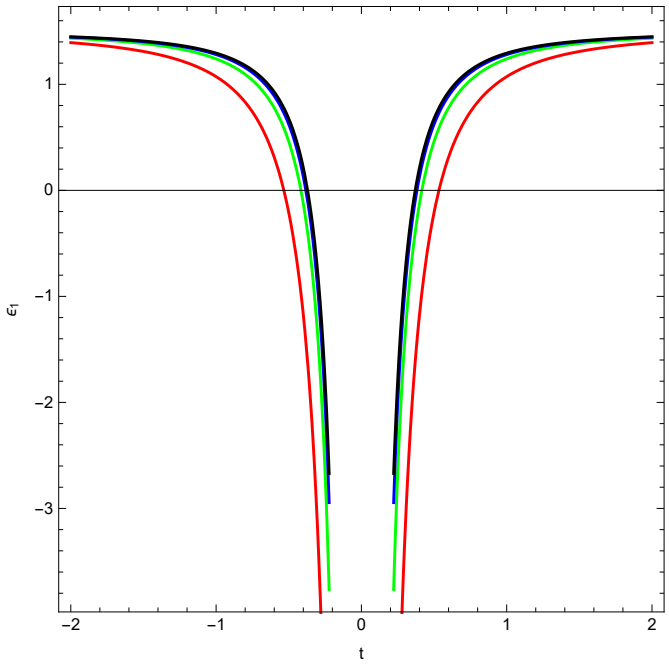

Figure 9. Hubble flow parameter ϵ_1 for the reconstructed mgCG density with time t.

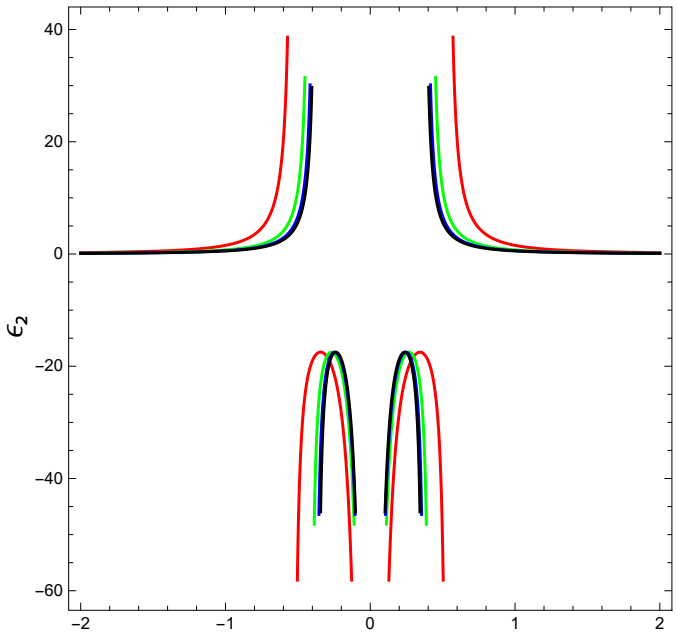

Figure 10. Hubble flow parameter ϵ_2 for the reconstructed mgCG density with time t.

5. Inflation via Scalar Field

In this section, we introduce a scalar field ϕ which is minimally coupled dependent on a potential $V(\phi)$ [143]. Therefore, in a curved space-time the Lagrangian [144] will be

$$\mathcal{L}_\phi = -\frac{1}{2}\mathcal{G}^{\alpha\beta}\partial_\alpha\phi\partial_\beta\phi - V(\phi). \tag{30}$$

Here, $\mathcal{G}^{\alpha\beta}$ is the metric tensor and $\partial_\alpha\phi$, $\partial_\beta\phi$ are covariant derivatives. Therefore, by considering the scalar field ϕ the effective mgCG energy density $\tilde{\rho_c}$ and the isotropic pressure incorporated with bulk viscosity will be

$$\tilde{\rho_c} = \frac{\dot{\phi}^2}{2} + V(\phi). \tag{31}$$

$$\tilde{p_c} = \frac{\dot{\phi}^2}{2} - V(\phi). \tag{32}$$

Now we want to demonstrate inflationary dynamics through the scalar field. In this present section, we considered a flat FRW universe filled with viscous mgCG in the scalar field framework. Taking $\tilde{\rho_c} = \rho$ for our background evolution of viscous mgCG, we have the following from Equations (31) and (32)

$$\dot{\phi}^2 = (1+\epsilon)\left(-12^{-\gamma}A(\frac{t^2\sigma^2}{(2+3t^2\sigma)^2})^{-\gamma} + \frac{12t^2\sigma^2}{(2+3t^2\sigma)^2}\right). \tag{33}$$

Hence,

$$\phi(t) = \sqrt{(1+\epsilon)}(\frac{2^{-\gamma}3^{-\gamma/2}\sqrt{A}t(1+\frac{3t^2\sigma}{2})^{-\gamma}(\frac{t^2\sigma^2}{(2+3t^2\sigma)^2})^{-\gamma/2}{}_2F_1\left[\frac{1-\gamma}{2}, -\gamma, 1+\frac{1-\gamma}{2}, -\frac{3t^2\sigma}{2}\right]}{-1+\gamma} + \frac{\sqrt{\frac{t^2\sigma^2}{(2+3t^2\sigma)^2}}(2+3t^2\sigma)\log\left[2+3t^2\sigma\right]}{\sqrt{3}t\sigma}). \tag{34}$$

Then, we can easily find the expression of $V(\phi(t))$. The basic purpose of this section is to demonstrate whether it is possible to have inflationary expansion from the viscous mgCG in scalar field formalism in a post-bounce scenario. Therefore, from Equations (31) and (32), we calculated this particular expression of potential.

$$V(\phi(t)) = \frac{1}{2}\left(12^{-\gamma}A(1+\epsilon)(\frac{t^2\sigma^2}{(2+3t^2\sigma)^2})^{-\gamma} - \frac{12t^2(-1+\epsilon)\sigma^2}{(2+3t^2\sigma)^2}\right). \tag{35}$$

We plotted non-singular $\dot{\phi}(t)$ in Figure 11 and the scalar field in Figure 12 respectively. So, the evolution of kinetic energy and the scalar field with cosmic time t is presented in Figure 11 and Figure 12, respectively. From Figure 12 we can show in the early universe, i.e., the pre-bounce scenario, the manner of the scalar field is decaying and rising in the later time of the universe. We have shown in Figure 13 the difference $v - \dot{\phi}^2$ and this figure is consistent with explaining inflationary expansion of the universe as $v > \dot{\phi}^2$ at the turnaround point and after the bounce scenario.

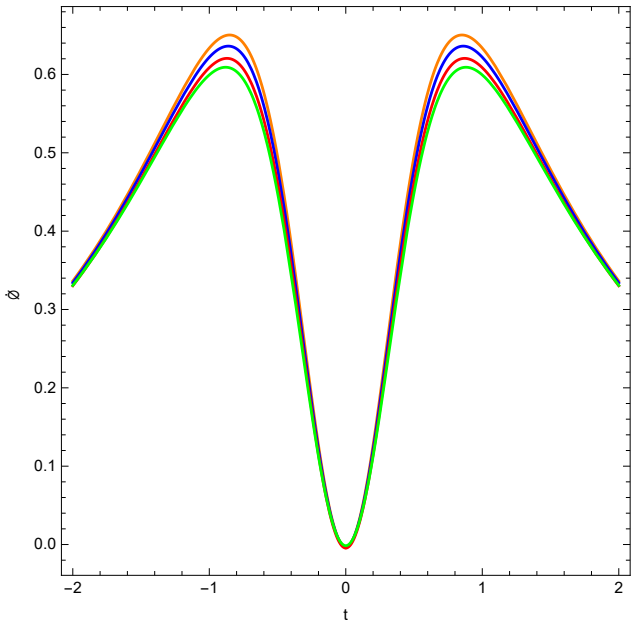

Figure 11. Evolution of kinectic energy with respect to cosmic time t.

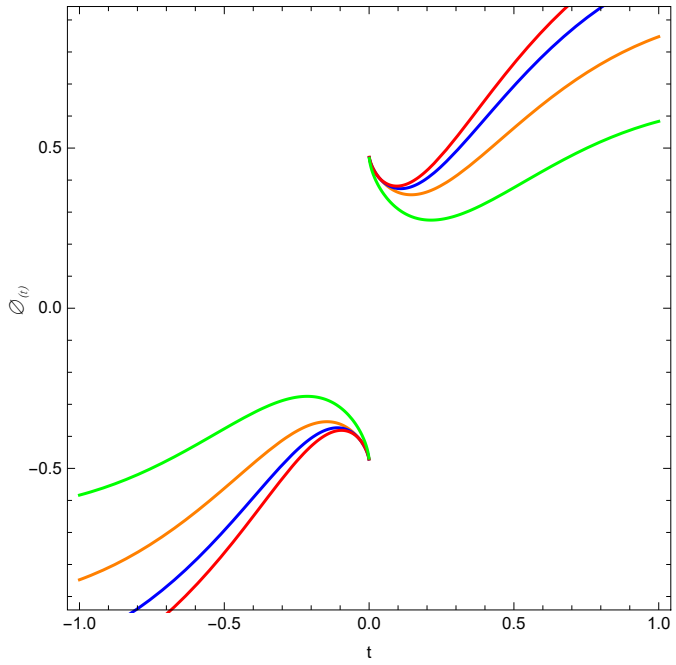

Figure 12. Evolution of scalar field $\phi(t)$ with respect to cosmic time t.

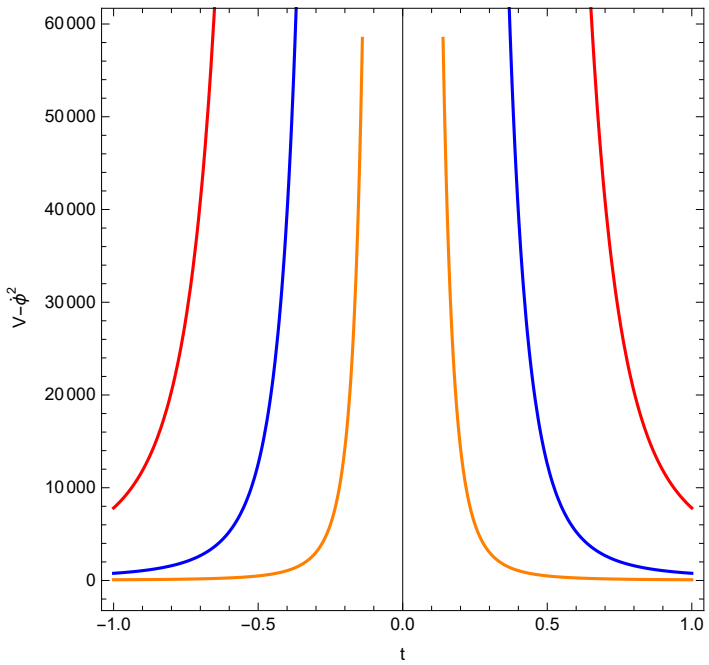

Figure 13. Evolution of $v - \dot{\phi}^2$ with respect to cosmic time t.

6. Fractional Density

In this section, we consider density parameter Ω. The definition of the density parameter is the ratio of the actual (or observed) density to the critical density of the Friedmann universe. Numerous studies explaining the expansion rate of the universe indicate that the universe is very close to reaching the critical density that would cause it to expand indefinitely. To study the expansion of the universe in a different way, we expressed the density as a fraction of the density required for the critical condition. To prove our universe is dominated by dark energy in this expansion era, we have studied fractional densities. The previous history of the Big Bang is viewed as being at first radiation dominated, then

matter dominated and now having passed into the era where dark energy is the dominant influence. Let us define the fractional densities [145]:

$$\Omega_{DE} = \frac{\rho_{mgCG}}{3H^2}. \tag{36}$$

$$\Omega_{DM} = \frac{\rho_m}{3H^2}. \tag{37}$$

$$\Omega_{DE} + \Omega_{DM} = 1. \tag{38}$$

Here, reconstructed Ω_{DM} and Ω_{DE} are as follows:

$$\Omega_{DM} = \frac{\rho_{m_0}(2 + 3t^2\sigma)}{12t^2\sigma^2}. \tag{39}$$

$$\Omega_{DE} = 1 - \frac{\rho_{m_0}(2 + 3t^2\sigma)}{12t^2\sigma^2}. \tag{40}$$

Here, we plotted the reconstructed fractional densities against cosmic time t in Figure 14 and it is clear that there is a transition from a matter dominated universe to an energy dominated universe. In the above figure, we can see dark matter is decreasing with time and dark energy is increasing with time with mgCG background evolution fluid.

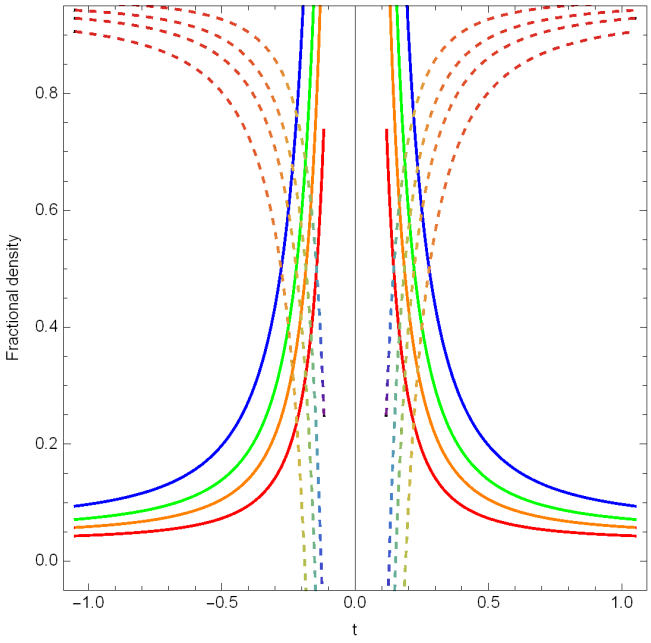

Figure 14. Evolution of fractional density with respect to cosmic time t with decreasing matter density shown by the solid-curve and increasing energy density by the dashed-curve with $\rho_{m_0} = 0.32$, $a_0 = 0.2$, $\epsilon = 0.43$, $\gamma = 0.89$ and $A = 0.96$ varying $\sigma = (2.34, 3.85, 4.56, 4.86)$ in units.

7. MGCG in *f(T)* Gravity

Here, introducing torsion T as a fundamental component [146], we considered "teleparallelism" connected with the Weitzenböck as a theory of gravity apart from Einstein's General Theory of Relativity. There are many cosmological studies (e.g., [147]), considered "teleparallelism" as a gravitational model with Lagrangian density as a function of T $[f(T)]$ to unify the inflationary epoch with the late time cosmological acceleration. In the study of Bamba et al. [148], finite-time future singularities have been studied with their thermodynamics. In the theory of modified teleparallel $f(T)$ gravity [149], the action I is given by

$$I = \frac{1}{16\pi G}\int d^4x\sqrt{-g}[f(T)] + \mathcal{L}_m. \tag{41}$$

Here, the matter Lagrangian density and gravitational constant are denoted by L_m and G, respectively, and g is the determinant of the metric tensor $g_{\mu v}$. In the exponential teleparallel $f(T)$ gravity scenario, by choosing energy density and pressure as ρ_m and p_m, respectively, the modified Friedmann equations are [150]

$$H^2 = \frac{\kappa^2}{3}(\rho_m + \rho_T). \tag{42}$$

$$2\dot{H} + 3H^2 = -\kappa^2(p_m + p_T). \tag{43}$$

Based on cosmological principles, the Big Bang theory is made up and from the Robertson–Walker metric; we can obtain the definition of κ, where κ is the spatial curvature, scaled so as to take the values 0 or ± 1. Here, we have taken the spherical universe and $\kappa = 1$.

Here, we constructed the $f(T)$ theory subject to bouncing scale factor by taking mgCG as the background evolution fluid of the universe.

$$\rho_T = \frac{1}{2\kappa^2}(2Tf' - f - T), \tag{44}$$

and

$$p_T = \frac{-2\dot{H}}{\kappa^2}[2Tf'' + f' - 1] - \rho_T. \tag{45}$$

In the above-stated equations, ρ_T and p_T are the Torsion contributed matter energy density and the pressure counterpart of standard ρ_m and p_m. We can write $f(T)$, f' and f'' in terms of cosmic time t easily. Therefore,

$$f' = \frac{\dot{f}}{\dot{T}}, \tag{46}$$

$$f'' = \frac{\dot{T}\ddot{f} - \ddot{T}\dot{f}}{\dot{T}^3}. \tag{47}$$

Here, the upper dot denotes the cosmic time derivative. For a pressureless dark matter $p_m = 0$ and the continuity equation can be integrated to $\rho_m = \rho_{m0}a^{-3}$.

$$f(t) = \frac{2\rho_{m_0} + 2\sqrt{6}\rho_{m_0}t\sqrt{\sigma}ArcTan\left[\sqrt{\frac{3}{2}}t\sqrt{\sigma}\right] + tC_1}{2 + 3t^2\sigma}. \tag{48}$$

In this case, for background evolution, we chose $\omega_T = \omega_{mgCG}$ in the bulk viscous scenario. Then, from Equation (3), we can write,

$$\omega_{mgCG} = \epsilon - (1+\epsilon)A\rho^{-\gamma-1}. \tag{49}$$

$$\omega_T = \omega_{mgCG}. \tag{50}$$

$$\rho_T = \frac{A(1+\epsilon)^{\frac{1}{\gamma+1}}}{\epsilon - \omega_T} = 12^{1+\gamma}\left(\frac{t^2\sigma^2}{(2+3t^2\sigma)^2}\right). \tag{51}$$

In Figure 15, we present the arbitrary torsion contributed function $f(t)$. The evolution of the reconstructed torsion contributed density is presented in Figure 16. where a symmetric pattern is observed around the bouncing point. In the pre-bounce scenario $f(t)$ has a decaying pattern and after bounce in the inflationary scenario $f(t)$ follows an increasing pattern. After the inflationary expanding era $f(t)$ regains its falling behavior. So, we can say this model shows realistic reconstruction. Figure 16 shows increasing energy density in both pre- and post-bounce scenarios and is continuous at $t = 0$ for $f(T)$ gravity also. However, after the inflation rho_T has a falling pattern tendency and then it remains stable for all values of σ. The torsion reconstructed EoS parameter is plotted in Figure 17. In the

pre-bounce scenario, at first the EoS parameter avoids Big Rip singularity by transiting from less than -1 to $\frac{-1}{3}$but t tends to the turnaround point again; it crosses the phantom boundary. In the inflationary era, there is a transition from less than -1 to $\frac{-1}{3}$ which is the avoidance of Big Rip singularity in the post-bounce scenario and afterwards again it crosses the phantom boundary in the later universe. However, w_T always has crossed $\frac{-1}{3}$ as required in accelerated expansion of the post-bounce scenario.

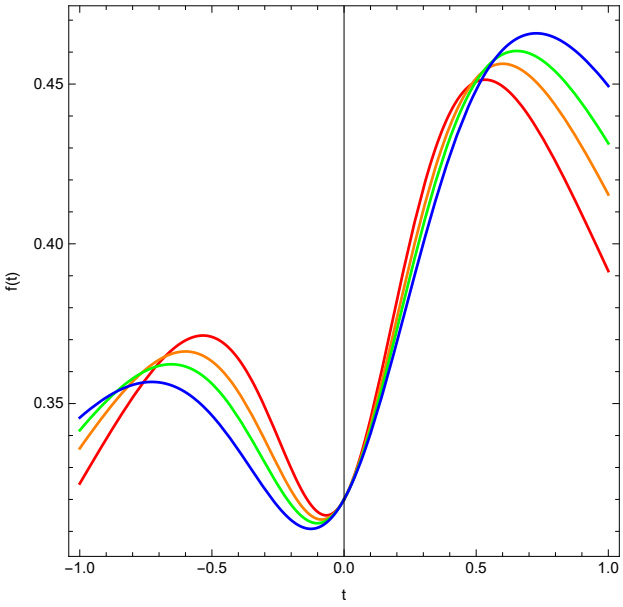

Figure 15. Reconstructed arbitrary torsion contributed function f evolution with respect to cosmic time t in the modified generalized Chaplygin Gas scenario with $\rho_{m_0} = 0.32$, $a_0 = 0.2$, $\epsilon = 0.43$, $\gamma = 0.89$ and $A = 0.96$ varying $\sigma = (2.34, 3.85, 4.56, 4.86)$ in units for orange-solid curve, red-solid curve, blue-solid curve and green-solid curve, respectively, with the bouncing point arising at $t = 0$.

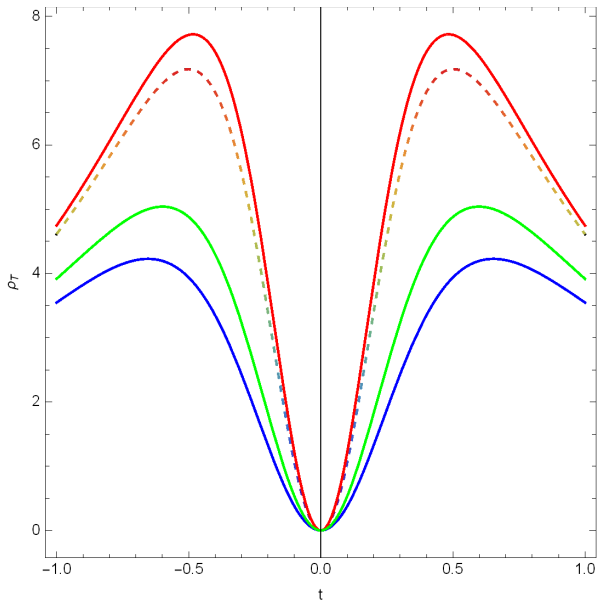

Figure 16. Reconstructed torsion contributed density evolution ρ_T in the modified generalized Chaplygin Gas scenario with $\rho_{m_0} = 0.32$, $a_0 = 0.02$, $\epsilon = 0.64$, $\gamma = 0.68$ and $A = 2.3$ varying $\sigma = (2.65, 2.85, 1.56, 1.86)$ in units for rainbow-dashed curve, red-solid curve, blue-solid curve and green-solid curve, respectively, with the bouncing point arising at $t = 0$.

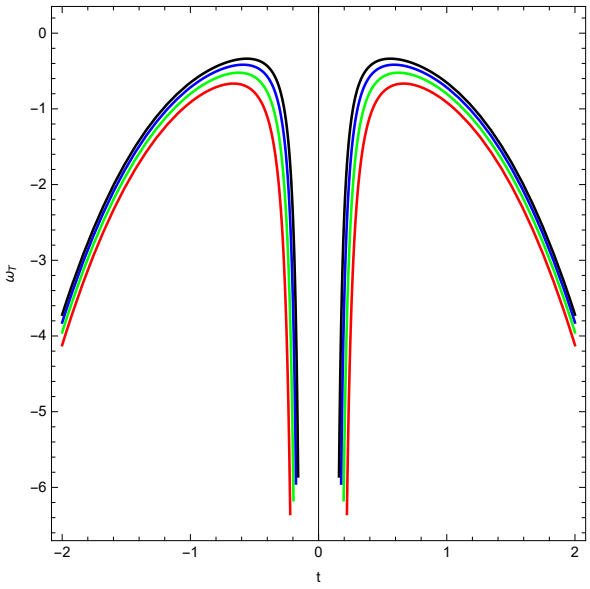

Figure 17. Reconstructed torsion contributed EoS parameter evolution ω_T in the modified generalized Chaplygin Gas scenario with $\rho_{m_0} = 0.32$, $a_0 = 0.2$, $\epsilon = 0.43$, $\gamma = 0.89$ and $A = 0.96$ varying $\sigma = (2.34, 3.85, 4.56, 4.86)$ in units for black-solid curve, red-solid curve, blue-solid curve and green-solid curve, respectively, with the bouncing point arising at $t = 0$.

8. Stability Analysis

Here, we have implemented a study on stability analysis in the framework of Einstein's as well as modified $f(T)$ gravity. Here, we used square speed of sound [151,152] to find the stability of the model.

$$V_s^2 = \frac{dp}{d\rho}. \tag{52}$$

The stability of the model depends on $V_s^2 \geq 0$. If the value is negative it shows instability of the model. Here, we incorporated the squared speed of sound for mgCG reconstruction schemes in Einstein's as well as modified $f(T)$ gravity scenario and plotted V_s^2 versus cosmic time t. In Figure 18, we plotted V_s^2 in Einstein's framework which is continuous and well behaved. In Figure 19, we present the stability analysis by plotting V_s^2 in a modified $f(T)$ gravity scenario. Here, for the $f(T)$ gravity scenario it diverges and does not exist near the turnaround point.

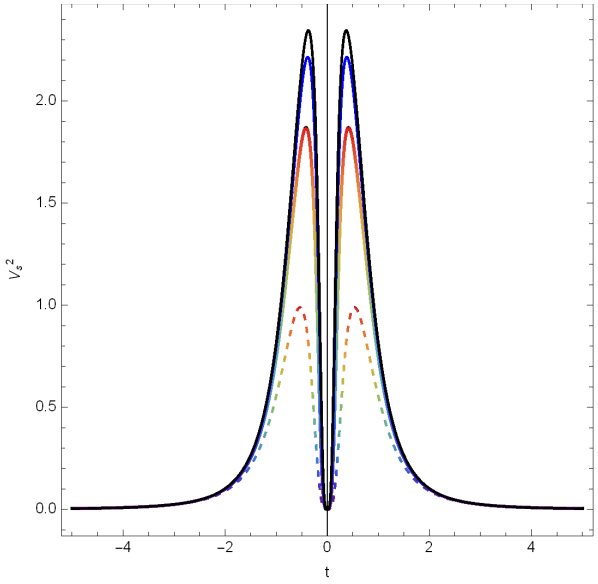

Figure 18. Evolution of square speed of sound $V_s^2 > 0$ for Einstein gravity scenario.

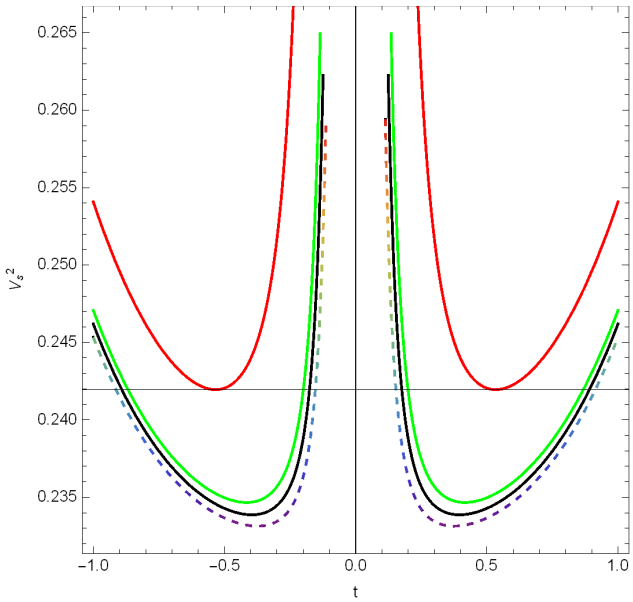

Figure 19. Evolution of square speed of sound $V_s^2 > 0$ for modified $f(T)$ gravity scenario.

The square speed of sound diverges at the bouncing point for the model in the $f(T)$ modified gravity framework although it is continuous in Einstein's gravity framework. This indicates the possible instability of the model at the bouncing point and requires further study.

9. Uncertainty Towards Bouncing Point

Here, we present a detailed study on observational $H(z)$ data from Luminous Red Galaxies of Sloan Digital Sky Survey Data Release Seven (SDSS DR7), which are available at [153]. Initially let us have a glance at the illustrative statistics related to the data set regarding the bouncing scenario. In the above stated dataset, we have Hubble data $H(z)$ with respect to redshift (z) data. We know that

$$\frac{1}{a(t)} = 1 + z, \tag{53}$$

where $a(t)$ refers to scale factor and z refers to the Hubble dataset. We converted the redshift dataset to cosmic time.

In the subsequent section, we present a rigorous study on finding uncertainty towards a bouncing point through a probabilistic information theory using the method of Shannon entropy maximization. Here, we applied the probabilistic information theory to obtain a deterministic picture of the uncertainty correlated with the evolution of the universe. The Shannon entropy quantifies the uncertainty associated with a stochastic variable explained in a given probability space. For this case, an entropy maximizing probability distribution is acquired by construction of Lagrangian [154]

$$\mathcal{L} = -\sum_{x=1}^{n} p_x \ln p_x - \alpha\left(\sum_{x=1}^{n} p_x - 1\right) - \beta\left(\sum_{x=1}^{n} p_x y_x - E(y)\right), \tag{54}$$

$$\frac{\partial \mathcal{L}}{\partial \alpha} = 1 - \sum_{x=1}^{n} p_x y_x, \tag{55}$$

$$\frac{\partial \mathcal{L}}{\partial \beta} = E(y) - \sum_{x=1}^{n} p_x y_x, \tag{56}$$

$$\frac{\partial \mathcal{L}}{\partial p_x} = -\ln p_x - 1 - \alpha - \beta y_x. \tag{57}$$

Solving the above equations, the entropy maximizing probability distribution becomes

$$p_x = \frac{\exp(-\beta y_x)}{\sum_{x=1}^{n} \exp(-\beta y_m)} \quad \text{where} \quad m = 1, 2, 3, \ldots, n \tag{58}$$

In Equation (58), the probabilities prevail in the manner explained above. It must be noted that β is attained through the Newton–Raphson method. This probability distribution is used to calculate the uncertainty in respect of Shannon entropy $H(p)$ as

$$H(p_1, p_2, p_3, \ldots, p_n) = -\sum_{x=1}^{n} p_x \ln p_x \tag{59}$$

Here, we varied the E[t], where t is the cosmic time. This adaptation is conducted by taking the cosmic time towards bouncing point from the pre-bounce scenario as well as from the post-bounce scenario. Appropriately, the entropy maximizing probability distribution was attained for all expectations. It should be mentioned that the values of β are attained through application of the Newton–Raphson method on the following equation

$$\sum_{x=1}^{n} (t_x - E(t)) \exp(-\beta t_x) = 0 \tag{60}$$

The variation of Shannon entropy with respect to cosmic time is presented in Figure 20. It is clear from Figure 20 that the uncertainty, computed through Shannon entropy, is lower at early times and it is greater near the turnaround point of the universe. After, the bounce uncertainty is higher as the inflationary expansion has occurred. As Shannon entropy is an estimation of randomness in a system, we observe that the uncertainty is reduced as we evolve from Big Bang inflationary to late time universe. Therefore, the reconstruction scheme presented here has the potential to be considered as a unifying model for early inflation and late time acceleration.

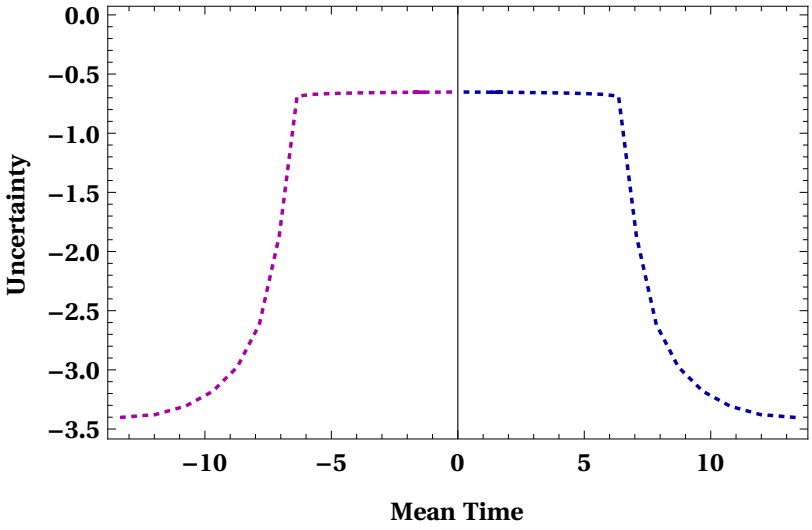

Figure 20. Uncertainty towards turnaround point.

From the Figure 20, we can see, at the very early contracting phase of the universe, uncertainty is very much less and after that uncertainty is increasing when cosmic time leads to the turnaround point. After that, at the inflationary era uncertainty is higher and later the universe uncertainty is decreasing at the post-bounce scenario.

10. Discussion and Concluding Remarks

In the concluding remarks, there are a few important points to be discussed. We started with modified generalized Chaplygin Gas (mgCG) as the background evolution.

The mgCG can interpolate the phases between standard pressure at high energy density fluids and negatively constant pressure with low density energy fluids by varying GCG to the mgCG [155]. The study of Zhang and Zhu [156] is the most relevant study in this framework of the manuscript, in which taking Chaplygin Gas to act as DE interacting with DM results in an EoS parameter (ω) in a bulk viscous scenario capable of crossing $\omega < -1$. Other references [156–160], which are relevant to this work, take a different variant of noninteracting Chaplygin Gas with a $f(T)$ reconstruction scheme and establish the necessary conditions for crossing the phantom boundary.

In this paper, we looked at a bouncing scale factor of the form $a(t) = a_0(\frac{1+3t^2\sigma}{2})^{\frac{1}{3}}$ where a_0 is the scale factor at the bouncing point and σ is a positive parameter describing the speed with which the bounce occurs. The bouncing point appeared at $t = 0$. This model realized big-bounce in the framework of Einstein gravity as well as $f(T)$ modified gravity, which violates the null energy condition (NEC) $p + \rho \geq 0$ for all values of σ. Incorporating the Friedmann equation, we derived the mgCG reconstructed density, the EoS parameter and the effective EoS parameter, respectively, and plotted them against cosmic time t. In the very first section of this manuscript, we plotted the reconstructed mgCG density evolution with respect to cosmic time t in Figure 1 and the figure supports the inflationary expansion of the universe; we can see in the figure that density increases due to inflation after the bounce and then remains stable in the later phase of the universe. Figure 1 shows non-singular bounce, which is a very obvious result of taking nonsingular scale factor and in Figure 2 we can see the EoS parameter crosses the phantom boundary but in Figure 5 avoidance of Big Rip has been demonstrated. Our next purpose was to show inflationary dynamics. In Figure 6, we used the e-folding time scale to calculate the time derivative of the e-fold number $\dot{N}$ versus time t and plotted it against the cosmic t. The scale factor at the bouncing point, $a = a_0$, has been shown to be $N = 0$. In Figure 6, $\dot{N}$ is symmetric about the bouncing time $t = 0$ and allows for nonsingular bounce realization. It is observed that before the bounce $t < 0$, $\dot{N} < 0$ due to universe contraction as a time-varying expansion factor $\dot{a} < 0$ and after the bounce $t > 0$, $\dot{N} > 0$ due to universe expansion. We plotted Hubble flow parameters in Figures 9 and 10. Figure 9 depicts an increasing pattern of ϵ_1 prior to the bounce. Following the bounce, $\epsilon_1 << 1$ meets the necessary condition for inflation. After that, it crosses the boundary of $\epsilon_1 = 1$ and indicates a nice exit from inflation. As a result, Figure 10 depicts the realization of inflation. In Figure 10, just before the bounce, $\epsilon_2 < 0$ is less than zero, supporting the inflationary theory and immediately after the bounce $H > 0$, ϵ_2 is less than zero, also supporting inflationary theory. Then, it becomes positive.

We have shown in Figure 12 the minimally coupled scalar field $\phi(t)$ and demonstrated its behavior. In the pre-bounce case, it behaves in a decaying manner and in a rising manner in the later time of the universe. We have shown in Figure 13 the difference $v - \dot{\phi}^2$ and this figure explains the inflationary expansion of the universe as $v > \dot{\phi}^2$ at the turnaround point and the post-bounce scenario as well. The fractional densities are plotted in Figure 14 and we can clearly understand the transition from DM domination to energy domination. In the next phase, we have shifted to a modified gravity framework which is chosen to be $f(T)$ gravity. The scale factor for this purpose has been chosen in bouncing form $a(t) = a_0(\frac{1+3t^2\sigma}{2})^{\frac{1}{3}}$. Our intention was to demonstrate the cosmology of $f(T)$ gravity where the function f, density ρ_T supports the inflationary cosmology of the universe by considering a correspondence between ω_c and ω_T. The torsion contributed EoS parameter always crosses $\frac{-1}{3}$ as required in accelerated expansion of the post-bounce scenario and it also supports inflationary cosmology. During the bounce, this model is stable in Einstein's and as well as the $f(T)$ modified gravity scenario against small perturbations. We checked the stability analysis of gravitational perturbations through square speed of sound.

Through the application of Shannon entropy, we analyzed the outcomes. The variation of Shannon entropy with cosmic time is presented in Figure 20. It is clear from Figure 20 that the uncertainty, computed through Shannon entropy, is lower at early stages of the universe. It is more significant in the later stage of the universe towards the turnaround point. After

the bounce, uncertainty is higher as the inflationary expansion has occurred. Shannon entropy is an estimation of randomness in a system. We observe that the uncertainty is reduced as we evolve from Big Bang inflationary to late time universe. Therefore, the reconstruction scheme presented here has the potential to be considered a unifying model for early inflation and late time acceleration.

While concluding, let us mention the newness of the current work with respect to some related works. First, let us mention the work by us in [161] where generalized Chaplygin Gas was studied in a $f(T)$ gravity framework and the Shannon entropy approach was adopted to optimize the uncertainty associated with the model. Contrary to [161], the current work is extended much further by focusing on the realization of cosmological bounce in a reconstruction scheme for modified gravity with modified generalized Chaplygin Gas as the background fluid. In this context, another relevant work by one of the authors of the current paper, namely "A study on the bouncing behavior of modified Chaplygin Gas in presence of bulk viscosity and its consequences in the modified gravity framework" where modified Chaplygin Gas is studied in $f(T)$ gravity for non-singular bounce, concentrating on the suitability of the bouncing scale factor in inflationary cosmology as well. The current work deviates much from [162] in the sense that here every cosmological consequence was throughly checked for pre-bounce and post-bounce scenarios. Furthermore, the Shannon entropy theory was extensively incorporated to visualize the uncertainty associated with the bouncing point with respect to pre-bounce contraction and post-bounce expansion. We hope to expand this research to include other types of modified gravity, as well as the baro holographic fluid.

Author Contributions: S.S.: Methodology, Formal analysis, Graph plotting, Writing—original draft, Graph plotting. S.C.: Writing—review and editing, Validation, Project administration. All authors have read and agreed to the published version of this manuscript.

Funding: This research received no external funding.

Data Availability Statement: Not applicable.

Acknowledgments: The authors are thankful to the anonymous reviewers for constructive suggestions.

Conflicts of Interest: The authors declare no conflict of interest.

References

1. Perlmutter, S.; Aldering, G.; Valle, M.D.; Deustua, S.; Ellis, R.S.; Fabbro, S.; Fruchter, A.; Goldhaber, G.; Groom, D.E.; Hook, I.M.; Kim, A.G. Discovery of a supernova explosion at half the age of the Universe. *Nature* **1998**, *391*, 51–54. [CrossRef]
2. Perlmutter, S.; Aldering, G.; Goldhaber, G.; Knop, R.A.; Nugent, ; Castro, G.; Deustua, S.; Fabbro, S.; Goobar, A.; Groom, D.E.; Hook, I.M. Measurements of Ω and Λ from 42 high-redshift supernovae. *Astrophys. J.* **1999**, *517*, 565. [CrossRef]
3. Riess, A.G.; Filippenko, A.V.; Challis, ; Clocchiatti, A.; Diercks, A.; Garnavich, M.; Gillil, ; R.L.; Hogan, C.J.; Jha, S.; Kirshner, R.P.; Leibundgut, B. Observational evidence from supernovae for an accelerating universe and a cosmological constant. *Astron. J.* **1998**, *116*, 1009. [CrossRef]
4. Riess, A.G.; Strolger, L.G.; Tonry, J.; Casertano, S.; Ferguson, H.C.; Mobasher, B.; Challis, P.; Filippenko, A.V.; Jha, S.; Li, W.; Chornock, R. Type Ia supernova discoveries at z > 1 from the Hubble Space Telescope: Evidence for past deceleration and constraints on dark energy evolution. *Astrophys. J.* **2004**, *607*, 665. [CrossRef]
5. Miller, A.D.; Caldwell, R.; Devlin, M.J.; Dorwart, W.B.; Herbig, T.; Nolta, M.R.; Page, L.A.; Puchalla, J.; Torbet, E.; Tran, H.T. A Measurement of the Angular Power Spectrum of the Cosmic Microwave Background from l = 100 to 400. *Astrophys. J.* **1999**, *524*, L1. [CrossRef]
6. Boisseau, B.; Esposito-Farese, G.; Polarski, D.; Starobinsky, A.A. Reconstruction of a scalar-tensor theory of gravity in an accelerating universe. *Phys. Rev. Lett.* **2000**, *85*, 2236. [CrossRef] [PubMed]
7. Bennett, C.L.; Larson, D.; Weil, ; J.L.; Jarosik, N.; Hinshaw, G.; Odegard, N.; Smith, K.M.; Hill, R.S.; Gold, B.; Halpern, M.; Komatsu, E. Nine-year Wilkinson Microwave Anisotropy Probe (WMAP) observations: Final maps and results. *Astrophys. J. Suppl. Ser.* **2013**, *208*, 20. [CrossRef]
8. Bennett, C.L.; Hill, R.S.; Hinshaw, G.; Larson, D.; Smith, K.M.; Dunkley, J.; Gold, B.; Halpern, M.; Jarosik, N.; Kogut, A.; Komatsu, E. Seven-year wilkinson microwave anisotropy probe (WMAP*) observations: Are there cosmic microwave background anomalies? *Astrophys. J. Suppl. Ser.* **2011**, *192*, 17. [CrossRef]

9. Larson, D.; Dunkley, J.; Hinshaw, G.; Komatsu, E.; Nolta, M.R.; Bennett, C.L.; Gold, B.; Halpern, M.; Hill, R.S.; Jarosik, N.; Kogut, A. Seven-year wilkinson microwave anisotropy probe (WMAP*) observations: power spectra and WMAP-derived parameters. *Astrophys. J. Suppl. Ser.* **2011**, *192*, 16. [CrossRef]
10. Bridle, S.L.; Lahav, O.; Ostriker, J.P.; Steinhardt, J. Precision cosmology? Not just yet... *Science* **2013**, *299*, 1532–1533. [CrossRef]
11. Spergel, D.N.; Verde, L.; Peiris, H.V.; Komatsu, E.; Nolta, M.R.; Bennett, C.L.; Halpern, M.; Hinshaw, G.; Jarosik, N.; Kogut, A.; Limon, M. First-year Wilkinson Microwave Anisotropy Probe (WMAP)* observations: determination of cosmological parameters. *Astrophys. J. Suppl. Ser.* **2003**, *148*, 175. [CrossRef]
12. Bahcall, N.A.; Ostriker, J.P.; Perlmutter, S.; Steinhardt, J . The cosmic triangle: Revealing the state of the universe. *Science* **1999**, *284*, 1481–1488. [CrossRef]
13. Tegmark, M.; Strauss, M.A.; Blanton, M.R.; Abazajian, K.; Dodelson, S.; Sandvik, H.; Wang, X.; Weinberg, D.H.; Zehavi, I.; Bahcall, N.A.; et al. Cosmological parameters from SDSS and WMAP. *Phys. Rev. D* **2004**, *69*, 103501. [CrossRef]
14. Anand, S.; Chaubal, P.; Mazumdar, A.; Mohanty, S. Cosmic viscosity as a remedy for tension between PLANCK and LSS data. *J. Cosmol. Astropart. Phys.* **2017**, *11*, 5. [CrossRef]
15. Ciarcelluti, P. Cosmology with mirror dark matter II: cosmic microwave background and large scale structure. *Int. J. Mod. Phys.* **2005**, *14*, 223–256. [CrossRef]
16. Willis, J.P.; Pacaud, F.; Valtchanov, I.; Pierre, M.; Ponman, T.; Read, A.; Andreon, S.; Altieri, B.; Quintana, H.; Dos, Santos, S.; Birkinshaw, M. The XMM Large-Scale Structure survey: An initial sample of galaxy groups and clusters to a redshift z < 0.6. *Mon. Not. R. Astron. Soc.* **2005**, *363*, 675–691.
17. Li, H.; Xia, J.Q. Constraints on dark energy parameters from correlations of CMB with LSS. *J. Cosmol. Astropart. Phys.* **2010**, *4*, 026. [CrossRef]
18. Amendola, L.; Tsujikawa, S. *Dark Energy: Theory and Observations*; Cambridge University Press: Cambridge, UK, 2010.
19. Hinshaw, G.; Weil, P.; J.L.; Hill, R.S.; Odegard, N.; Larson, D.; Bennett, C.L.; Dunkley, J.; Gold, B.; Greason, M.R.; Jarosik, N.; et al. Five-year wilkinson microwave anisotropy probe* observations: Data processing, sky maps and basic results. *Astrophys. J. Suppl. Ser.* **2009**, *180*, 225. [CrossRef]
20. Rahaman, F. *The General Theory of Relativity: A Mathematical Approach*; Cambridge University Press, University Printing House: Cambridge, UK, 2021.
21. Anderson, J.L. General Relativity: Gravitation and Cosmology. Principles and Applications of the General Theory of Relativity. Steven Weinberg. Wiley, New York. *Science* **1973**, *179*, 1227–1228. [CrossRef]
22. Weinberg, S. Cosmological production of baryons. *Phys. Rev. Lett.* **1979**, *42*, 850. [CrossRef]
23. Crispino, L.C.; Kennefick, D.J. A hundred years of the first experimental test of general relativity. *Nat. Phys.* **2019**, *15*, 416-419. [CrossRef]
24. Synge, J.L.; Romain, J. Relativity: The general theory. *Phys. Today* **1961** , *14*, 50. [CrossRef]
25. Colistete Jr, R.; Fabris, J.C.; Tossa, J.; Zimdahl, W. Bulk viscous cosmology. *Phys. Rev. D.* **2007**, *76*, 103516. [CrossRef]
26. Martin, J. Everything you always wanted to know about the cosmological constant problem (but were afraid to ask). *C. R. Phys.* **2012**, *13*, 566–665. [CrossRef]
27. Padilla, A. Lectures on the cosmological constant problem. *arXiv* **2015**, arXiv:1502.05296.
28. Weinberg, S. The cosmological constant problem. *Rev. Mod. Phys.* **1989**, *61*, 1. [CrossRef]
29. Zel'dovich, Y.B. The cosmological constant and the theory of elementary particles. *Sov. Phys. USP* **1968**, *11*, 11381–11393
30. Sahni, V.; Krasiński, A. Republication of: The cosmological constant and the theory of elementary particles (By Ya. B. Zeldovich). *Gen. Relativ. Gravit.* **2008**, *40*, 1557–1591. [CrossRef]
31. Padmanabhan, T. Cosmological constant—The weight of the vacuum. *Phys. Rep.* **2003**, *380*, 235–320. [CrossRef]
32. Wu, J.P.; Ma, D.Z.; Ling, Y. Quintessence reconstruction of the new agegraphic dark energy model. *Phys. Lett.* **2008**, *663*, 152–159. [CrossRef]
33. Dutta, S.; Saridakis, E.N.; Scherrer, R.J. Dark energy from a quintessence (phantom) field rolling near a potential minimum (maximum). *Phys. Rev.* **2009**, *79*, 103005. [CrossRef]
34. Cai, Y.F.; Saridakis, E.N.; Setare, M.R.; Xia, J.Q. Quintom cosmology: Theoretical implications and observations. *Phys. Rep.* **2010**, *493*, 1–60. [CrossRef]
35. Debnath, U.; Chattopadhyay, S.; Hussain, I.; Jamil, M.; Myrzakulov, R. Generalized second law of thermodynamics for FRW cosmology with power-law entropy correction. *Eur. Phys. J.* **2012**,*72*, 1–6. [CrossRef]
36. Nojiri, S.I.; Odintsov, S.D.; Tsujikawa, S. Properties of singularities in the (phantom) dark energy universe. *Phys. Rev.* **2005**, *71*, 063004. [CrossRef]
37. Vikman, A. Can dark energy evolve to the phantom? *Phys. Rev. D* **2005**, *71*, 023515. [CrossRef]
38. Nojiri, S.I.; Odintsov, S.D. Quantum de Sitter cosmology and phantom matter. *Phys. Lett.* **2003**, *562*, 147–152. [CrossRef]
39. Elizalde, E.; Nojiri, S.I.; Odintsov, S.D. Late-time cosmology in a (phantom) scalar-tensor theory: Dark energy and the cosmic speed-up. *Phys. Rev.* **2004**, *70*, 043539. [CrossRef]
40. Sami, M.; Toporensky, A.; Tretjakov, V.; Tsujikawa, S. The fate of (phantom) dark energy universe with string curvature corrections. *Phys. Lett.* **2005**, *619*, 193–200. [CrossRef]
41. Nojiri, S.I.; Odintsov, S.D. Final state and thermodynamics of a dark energy universe. *Phys. Rev.* **2004**, *70*, 103522. [CrossRef]

42. Guo, Z.K.; Piao, Y.S.; Zhang, X.; Zhang, Y.Z. Cosmological evolution of a quintom model of dark energy. *Phys. Lett.* **2005**, *608*, 177–182. [CrossRef]
43. Cai, Y.F.; Li, M.; Lu, J.X.; Piao, Y.S.; Qiu, T.; Zhang, X. A string-inspired quintom model of dark energy. *Phys. Lett.* **2007**, *651*, 1–7. [CrossRef]
44. Zhao, G.B.; Xia, J.Q.; Li, M.; Feng, B.; Zhang, X. Perturbations of the quintom models of dark energy and the effects on observations. *Phys. Rev.* **2005**, *72*, 123515. [CrossRef]
45. Feng, B.; Li, M.; Piao, Y.S.; Zhang, X. Oscillating quintom and the recurrent universe. *Phys. Lett.* **2006**, *634*, 101–105. [CrossRef]
46. Bagla, J.S.; Jassal, H.K.; Padmanabhan, T. Cosmology with tachyon field as dark energy. *Phys. Rev.* **2003**, *67*, 063504. [CrossRef]
47. Setare, M.R.; Sadeghi, J.; Amani, A.R. Interacting tachyon dark energy in non-flat universe. *Phys. Lett.* **2009**, *673*, 241–246. [CrossRef]
48. Copel, ; E.J.; Garousi, M.R.; Sami, M.; Tsujikawa, S. What is needed of a tachyon if it is to be the dark energy? *Phys. Rev.* **2005**, *71*, 043003.
49. Wei, H.; Cai, R.G.; Zeng, D.F. Hessence: A new view of quintom dark energy. *Class. Quantum Gravity* **2005**, *22*, 3189. [CrossRef]
50. Alimohammadi, M.; Sadjadi, H.M. Attractor solutions for general hessence dark energy. *Phys. Rev.* **2006**, *73*, 083527. [CrossRef]
51. Chimento, L.P. Extended tachyon field, Chaplygin Gas and solvable k-essence cosmologies. *Phys. Rev.* **2004**, *69*, 123517.
52. Gorini, V.; Kamenshchik, A.; Moschella, U.; Pasquier, V. The Chaplygin Gas as a model for dark energy. In *The Tenth Marcel Grossmann Meeting: On Recent Developments in Theoretical and Experimental General Relativity, Gravitation and Relativistic Field Theories (In 3 Volumes)*; World Scientific Publishing Company: Singapore, 2008; pp. 840–859. .
53. Saha, P.; Debnath, U. Study of anisotropic compact stars with quintessence field and modified chaplygin gas in f (T) gravity. *Eur. Phys. J. C* **2019**, *79*, 1–16. [CrossRef]
54. Setare, M.R. Holographic Chaplygin DGP cosmologies. *Int. J. Mod. Phys.* **2009**, *18*, 419–427. [CrossRef]
55. Avelino, P.; Bolejko, K.; Lewis, G.F. Nonlinear Chaplygin Gas cosmologies. *Phys. Rev.* **2014**, *89*, 103004. [CrossRef]
56. Li, M. A model of holographic dark energy. *Phys. Lett.* **2004**, **603**, 1–5. [CrossRef]
57. Elizalde, E.; Nojiri, S.I.; Odintsov, S.D.; Wang, P. Dark energy: Vacuum fluctuations, the effective phantom phase and holography. *Phys. Rev.* **2005**, *71*, 103504. [CrossRef]
58. Jamil, M.; Saridakis, E.N.; Setare, M.R. Holographic dark energy with varying gravitational constant. *Phys. Lett.* **2009**, *679*, 172–176. [CrossRef]
59. Chattopadhyay, S.; Debnath, U.; Holographic dark energy scenario and variable modified Chaplygin Gas. *Astrophys. Space Sci.* **2009**, *319*, 183–185. [CrossRef]
60. Bamba, K.; Capozziello, S.; Nojiri, S.I.; Odintsov, S.D. Dark energy cosmology: The equivalent description via different theoretical models and cosmography tests. *Astrophys. Space Sci.* **2012**, *342*, 155–228. [CrossRef]
61. Debnath, U.; Chattopadhyay, S. Statefinder and Om diagnostics for interacting new holographic dark energy model and generalized second law of thermodynamics. *Int. J. Theor. Phys.* **2013**, *52*, 1250–1264. [CrossRef]
62. Ghosh, R.; Pasqua, A.; Chattopadhyay, S. Generalized second law of thermodynamics in the emergent universe for some viable models of $f(T)$ gravity. *Eur. Phys. J. Plus* **2013**, *128*, 1–11. [CrossRef]
63. Saridakis, E.N.; Basilakos, S. The generalized second law of thermodynamics with Barrow entropy. *Eur. Phys. J.* **2021**, *81*, 1–6. [CrossRef]
64. Singh, C.P.; Kumar, A. Viscous Ricci dark energy and generalized second law of thermodynamics in modified $f(R, T)$ gravity. *Mod. Phys. Lett.* **2018**, *33*, 1850225. [CrossRef]
65. Benaoum, H. Accelerated universe from modified Chaplygin Gas and tachyonic fluid. *Universe* **2022**, *8*, 340. [CrossRef]
66. Polarski, D. Dark energy. *Int. J. Mod. Phys. D* **2013**, *22*, 1330027. [CrossRef]
67. Straumann, N. Dark energy: Recent developments. *Mod. Phys. Lett. A* **2008**, *21*, 1083–1098. [CrossRef]
68. Yoo, J.; Watanabe, Y. Theoretical models of dark energy. *Int. J. Mod. Phys. D* **2021**, *21*, 1230002. [CrossRef]
69. Sahni, V.; Starobinsky, A. Reconstructing dark energy. *Int. J. Mod. Phys. D* **2006**, *15*, 2105–2132. [CrossRef]
70. Sahni, V.; Shafieloo, A.; Starobinsky, A.A. Model-independent evidence for dark energy evolution from Baryon acoustic oscillations. *Astrophys. J. Lett.* **2014**, *793*, L40. [CrossRef]
71. Spergel, D.N.; Steinhardt, J. Observational evidence for self-interacting cold dark matter. *Phys. Rev. Lett.* **2000**, *84*, 3760. [CrossRef]
72. Liddle, A.R.; Lyth, D.H. The Cold dark matter density perturbation. *Phys. Rep.* **1993**, *231*, 1–105. [CrossRef]
73. Amendola, L.; Finelli, F.; Burigana, C.; Carturan, D. WMAP and the generalized Chaplygin Gas. *J. Cosmol. Astropart. Phys.* **2003**, *2003*, 005. [CrossRef]
74. Setare, M.R. Interacting holographic generalized Chaplygin gas model. *Phys. Lett. B* **2007**, *654*,1–6. [CrossRef]
75. Gorini, V.; Kamenshchik, A.; Moschella, U. Can the Chaplygin Gas be a plausible model for dark energy? *Phys. Rev.* **2003**, *67*, 063509. [CrossRef]
76. Kamenshchik, A.; Moschella, U.; Pasquier, V. An alternative to quintessence. *Phys. Lett. B* **2001**, *511*, 265–268 [CrossRef]
77. Bento, M.C.; Bertolami, O.; Sen, A. Generalized Chaplygin Gas, accelerated expansion and dark Energy-Matter unification. *Phys. Rev. D* **2002**, *66*, 043507. [CrossRef]
78. Bento, M.D.C.; Bertolami, O.; Sen, A.A. Generalized Chaplygin Gas and cosmic microwave background radiation constraints. *Phys. Rev.* **2003**, *67*, 063003. [CrossRef]
79. Sen, A.A.; Scherrer, R.J. Generalizing the generalized Chaplygin Gas. *Phys. Rev.* **2005**, *72*, 063511. [CrossRef]

80. Pun, C.S.J.; Gergely, L.; Mak, M.K.; Kovcs, Z.; Szab, G.M.; Harko, T. Viscous dissipative Chaplygin Gas dominated homogenous and isotropic cosmological models. *Phys. Rev. D* **2008**, *77*, 063528. [CrossRef]
81. Debnath, U.; Banerjee, A.; Chakraborty, S. Role of modified Chaplygin Gas in accelerated universe. *Class. Quantum Grav.* **2004**, *21*, 5609. [CrossRef]
82. Pourhassan, B. Viscous modified cosmic Chaplygin Gas cosmology. *Int. J. Mod. Phys. D* **2013**, *22*, 1350061 [CrossRef]
83. Chattopadhyay, S. Modified Chaplygin Gas equation of state on viscous dissipative extended holographic Ricci dark energy and the cosmological consequences. *Int. J. Mod. Phys. D* **2017**, *26*, 1750042. [CrossRef]
84. Jawad, A.; Ilyas, A.; Rani, S. Dynamics of modified Chaplygin Gas inflation on the Brane with bulk viscous pressure. *Int. J. Mod. Phys. D* **2017**, *26*, 1750031 [CrossRef]
85. Bedran, M.L.; Soares, V.; Araujo, M.E. Temperature evolution of the FRW universe filled with modified Chaplygin Gas. *Phys. Lett.* **2008**, *659*, 462–465. [CrossRef]
86. Panigrahi, D.; Chatterjee, S. Thermodynamics of the variable modified Chaplygin Gas. *J. Cosmol. Astropart. Phys.* **2016**, *2016*, 052. [CrossRef]
87. Salti, M.; Kangal, E.E.; Aydogdu, O. Variable Polytropic gas cosmology. *Ann. Phys.* **2019**, *407*, 166–178. [CrossRef]
88. Kamenshchik, A.Y.; Tronconi, A.; Venturi, G. Reconstruction of scalar potentials in induced gravity and cosmology. *Phys. Lett. B* **2011**, *702*, 191–196. [CrossRef]
89. Gorbunov, D.S.; Rubakov, V.A. *Introduction to the Theory of the Early Universe*; World Scientific: Singapore, 2018.
90. Odintsov, S.D.; Oikonomou, V.K. Deformed matter bounce with dark energy epoch. *Phys. Rev. D* **2016**, *94*, 064022. [CrossRef]
91. Nojiri, S.; Odintsov, S.D. Modified gravity with negative and positive powers of the curvature: Unification of the inflation and of the cosmic acceleration. *Phys. Rev. D* **2003**, *68*, 123512. [CrossRef]
92. Capozziello, S.; Nojiri, S.; Odintsov, S.D. Unified phantom cosmology: Inflation, dark energy and dark matter under the same standard. *Phys. Lett. B* **2006**, *632*, 597–604. [CrossRef]
93. Huang, Q.G.; Li, M. The holographic dark energy in a non-flat universe. *J. Cosmol. Astropart. Phys.* **2004**, *2004*, 013. [CrossRef]
94. Wang, B.; Gong, Y.; Abdalla, E. Transition of the dark energy equation of state in an interacting holographic dark energy model. *Phys. Lett.* **2005**, *624*, 141–146. [CrossRef]
95. Cai, Y.F. Exploring bouncing cosmologies with cosmological surveys. *Sci. China Phys. Mech. Astron.* **2014**, *57*, 1414–1430. [CrossRef]
96. Mukhanov, V.F.; Feldman, H.A.; Brandenberger, R.H. Theory of cosmological perturbations. *Phys. Rep.* **1992**, *215*, 203–333. [CrossRef]
97. Nojiri, S.; Odintsov, S.D.; Oikonomou, V. Modified gravity theories on a nutshell: inflation, bounce and late-time evolution. *Phys. Rep.* **2017**, *692*, 1–104. [CrossRef]
98. Bamba, K.; Makarenko, A.N.; Myagky, A.N.; Nojiri, S.I.; Odintsov, S.D. Bounce cosmology from F (R) gravity and F (R) bigravity. *J. Cosmol. Astropart. Phys.* **2014**, *2014*, 008. [CrossRef]
99. Bamba, K.; Odintsov, S.D. Inflationary cosmology in modified gravity theories. *Symmetry* **2015**, *7*, 220–240. [CrossRef]
100. Nojiri, S.I.; Odintsov, S.D.; Saridakis, E.N. Holographic bounce. *Nucl. Phys.* **2019**, *949*, 114790. [CrossRef]
101. Elizalde, E.; Nojiri, S.; Odintsov, S.D.; Sez-Gmez, D.; Faraoni, V. Reconstructing the universe history, from inflation to acceleration, with phantom and canonical scalar fields. *Phys. Rev. D* **2008**, *77*, 106005 [CrossRef]
102. Odintsov, S.D.; Paul, T. Bounce universe with finite-time singularity. *Universe* **2022**, *8*, 292. [CrossRef]
103. Nojiri, S.I.; Odintsov, S.D.; Paul, T. Towards a smooth unification from an ekpyrotic bounce to the dark energy era. *Phys. Dark Universe* **2022**, *35*, 100984. [CrossRef]
104. Capozziello, S.; De Laurentis, M. Extended theories of gravity. *Phys. Rep.* **2011**, *509*, 167-321. [CrossRef]
105. Barrow, J.D.; Graham, A.A. Singular inflation. *Phys. Rev.* **2015**, *91*, 083513. [CrossRef]
106. Nojiri, S.; Odintsov, S.D.; Oikonomou, V.K. Quantitative analysis of singular inflation with scalar-tensor and modified gravity. *Phys. Rev.* **2015**, *91*, 084059. [CrossRef]
107. Nojiri, S.; Odintsov, S.D.; Oikonomou, V.K. Singular inflation from generalized equation of state fluids. *Phys. Lett.* **2015**, *747*, 310–320. [CrossRef]
108. Barrow, J.D. Sudden future singularities. *Class. Quantum Gravity* **2004**, *21*, L79. [CrossRef]
109. Weinberg, S. Entropy generation and the survival of protogalaxies in an expanding universe. *Astrophys. J.* **1971**, *168*, 175 [CrossRef]
110. Clifton, T.; Barrow, J.D. The power of general relativity. *Phys. Rev. D* **2005**, *72*, 103005 . [CrossRef]
111. Medina, S.B., Nowakowski, M.; Batic, D. Viscous cosmologies. *Class. Quantum Gravity* **2019**, *36*, 215002. [CrossRef]
112. Jaffe, R.L. Casimir effect and the quantum vacuum. *Phys. Rev.* **2005**, *72*, 021301. [CrossRef]
113. Myrzakulov, R.; Sebastiani, L. Bounce solutions in viscous fluid cosmology. *Astrophys. Space Sci.* **2014**, *352*, 281–288. [CrossRef]
114. Brevik, I.; Timoshkin, A.V. Viscous fluid holographic bounce. *Int. J. Geom. Methods Mod. Phys.* **2020**, *17*, 2050023. [CrossRef]
115. Cataldo, M.; Cruz, N.; Lepe, S. Viscous dark energy and phantom evolution. *Phys. Lett.* **2005**, *619*, 5–10. [CrossRef]
116. Hu, M.G.; Meng, X.H. Bulk viscous cosmology: Statefinder and entropy. *Phys. Lett.* **2006**, *635*, 186–194. [CrossRef]
117. Clifton, T.; Ferreira, G.; Padilla, A.; Skordis, C. Modified gravity and cosmology. *Phys. Rep.* **2012**, *513*, 1–189. [CrossRef]
118. Nojiri, S.I.; Odintsov, S.D. Introduction to modified gravity and gravitational alternative for dark energy. *Int. J. Geom. Methods Mod. Phys.* **2007**, *4*, 115–145. [CrossRef]
119. Tsujikawa, S. Modified gravity models of dark energy. In *Lectures on Cosmology*; Springer: Berlin/Heidelberg, Germany, 2010; pp. 99–145.

120. Josset, T., Perez, A. and Sudarsky, D Dark energy from violation of energy conservation. *Phys. Rev. Lett.* **2008**, *118*, 021102. [CrossRef] [PubMed]
121. Myrzakulov, R. Accelerating universe from F (T) gravity. *Eur. Phys. J. C* **2011**, *71*, 1752. [CrossRef]
122. Chattopadhyay, S.; Pasqua, A. Reconstruction of $f(T)$ gravity from the Holographic dark energy. *Astrophys. Space Sci.* **2012**, *344*, 269–274. [CrossRef]
123. Joyce, A.; Lombriser, L.; Schmidt, F. Dark energy vs. modified gravity. *arXiv* **2016**, arXiv:1601.06133.
124. Bertschinger, E.; Zukin, P. Distinguishing modified gravity from dark energy. *Phys. Rev.* **2008**, *78*, 024015. [CrossRef]
125. Wang, Y. Differentiating dark energy and modified gravity with galaxy redshift surveys. *J. Cosmol. Astropart. Phys.* **2008**, *2008*, 021. [CrossRef]
126. Capozziello, S.; Matsumoto, J.; Nojiri, S.I.; Odintsov, S.D. Dark energy from modified gravity with Lagrange multipliers. *Phys. Lett.* **2010**, *693*, 198–208. [CrossRef]
127. Hu, W.; Sawicki, I. Parametrized post-Friedmann framework for modified gravity. *Phys. Rev.* **2007**, *76*, 104043. [CrossRef]
128. Nojiri, S.I.; Odintsov, S.D. Modified gravity and its reconstruction from the universe expansion history. *J. Phys. Conf. Ser.* **2007**, *66*, 012005. [CrossRef]
129. Sanders, R. VModified gravity without dark matter. *The Invisible Universe: Dark Matter and Dark Energy*: Springer: Berlin/Heidelberg, Germany, 2007; pp. 375–402.
130. Klir, G.J.; Folger, T.A. *Fuzzy Sets, Uncertainty and Information*; Prentice-Hall, Inc.: Hoboken, NJ, USA, 1987.
131. Witten, E. A mini-introduction to information theory. *Riv. Del Nuovo C.* **2020**, *43*, 187–227. [CrossRef]
132. Crupi, V.; Nelson, J.D.; Meder, B.; Cevolani, G.; Tentori, K. Generalized information theory meets human cognition: Introducing a unified framework to model uncertainty and information search. *Cogn. Sci.* **2018**, *42*, 1410–1456. [CrossRef] [PubMed]
133. Amani, A.R.Pourhassan, B. Viscous generalized Chaplygin gas with arbitrary. *Int. J. Theor. Phys.* **2013**, *52*, 1309-1313 [CrossRef]
134. Saha, S.; Chattopadhyay, S. Exploring of the summer monsoon rainfall around the Himalayas in time domain through maximization of Shannon entropy. *Theor. Appl. Climatol.* **2020**, *141*, 133–141. [CrossRef]
135. Klir, G.J. Uncertainty and information: foundations of generalized information theory. *Kybernetes* **2006**, *35*, 1297–1299. [CrossRef]
136. Cai, Y.-F.; Chen, S.-H.; Dent, J.B.; Dutta, S.; Saridakis, E.N. Matter bounce cosmology with the $f(T)$ gravity. *Class. Quantum Grav.* **2011**, *28*, 215011. [CrossRef]
137. Maartens, R. Dissipative cosmology. *Class. Quantum Gravity* **1995**, *12*, 1455. [CrossRef]
138. Albrecht, A.; Magueijo, J. Time varying speed of light as a solution to cosmological puzzles. *Phys. Rev.* **1999**, *59*, 043516. [CrossRef]
139. Padmanabhan, T. Emergent perspective of gravity and dark energy. *Res. Astron. Astrophys.* **2012**, *12*, 891. [CrossRef]
140. Coone, D.; Roesta, D.; Venninc, V. The Hubble flow of plateau inflation. *J. Cosmol. Astrophys.* **2015**, *1511*, 010. [CrossRef]
141. Hoffman, M.B.; Turner, M.S. Kinematic constraints to the key inflationary observables. *Phys. Rev. D* **2001**, *64*, 023506 [CrossRef]
142. Kinney, W.H. Inflation: Flow, fixed points and observables to arbitrary order in slow roll. *Phys. Rev. D* **2002**, *66*, 083508. [CrossRef]
143. Nojiri, S.I.; Odintsov, S.D. Unifying phantom inflation with late-time acceleration: Scalar phantom–non-phantom transition model and generalized holographic dark energy. *Gen. Relativ. Gravit.* **2006**, *38*, 1285–1304. [CrossRef]
144. Sahni, V.; Saini, T.D.; Starobinsky, A.A.; Alam, U. Statefinder—A new geometrical diagnostic of dark energy. *J. Exp. Theor. Phys. Lett.* **2003**, *77*, 201–206. [CrossRef]
145. Lam, Y.M.P. Perturbation Lagrangian theory for scalar fields-Ward-Takahashi identity and current algebra. *Phys. Rev.* **1972**, *6*, 2145. [CrossRef]
146. Paliathanasis, A., Barrow, J.D.; Leach, P.G.L. Cosmological solutions of f (T) gravity. *Phys. Rev. D* **2016**, *94*, 023525. [CrossRef]
147. Chattopadhyay, S.; Chakraborty, G. A reconstruction scheme for f (T) gravity: Variable generalized Chaplygin dark energy gas form. *Astron. Nachrichten* **2021**, *342*, 103–109. [CrossRef]
148. Abdalla, M.C.B.; Nojiri, S.I.; Odintsov, S.D. Consistent modified gravity: Dark energy, acceleration and the absence of cosmic doomsday.*Class. Quantum Gravity* **2005**, *22*, L35. [CrossRef]
149. Cai, Y.F., Capozziello, S., De Laurentis, M.; Saridakis, E.N. f (T) teleparallel gravity and cosmology. *Rep. Prog. Phys.* **2016**, *79*, 106901. [CrossRef] [PubMed]
150. Capozziello, S.; Nojiri, S.; Odintsov, S.D. Dark energy: The equation of state description versus scalar-tensor or modified gravity. *Phys. Lett.* **2006**, *634*, 93–100. [CrossRef]
151. Setare, M.R. Interacting holographic dark energy model in non-flat universe. *Phys. Lett.* **2006**, *642*, 1–4. [CrossRef]
152. Hannestad, S. Constraints on the sound speed of dark energy. *Phys. Rev.* **2005**, *71*, 103519. [CrossRef]
153. Zhang, C., Zhang, H., Yuan, S., Liu, S., Zhang, T.J. and Sun, Y.C.; Four new observational H (z) data from luminous red galaxies in the Sloan Digital Sky Survey data release seven. *Res. Astron. Astrophys.* **2014**, *14*, 1221. [CrossRef]
154. Chattopadhyay, S.; Chattopadhyay, G.; Midya, S.K. Shannon entropy maximization supplemented by neurocomputing to study the consequences of a severe weather phenomenon on some surface parameters. *Nat. Hazards* **2018**, *93*, 237–247. [CrossRef]
155. Aziza, A.; Chakraborty, G.; Chattopadhyay, S. Variable generalized Chaplygin gas in f (Q) gravity and the inflationary cosmology. *Int. J. Mod. Phys. D* **2021**, *30*, 2150119. [CrossRef]
156. Jamil, M.; Myrzakulov, Y.; Razina, O.; Myrzakulov, R. Modified Chaplygin Gas and solvable F-essence cosmologies. *Astrophys. Space Sci.* **2011**, *336*, 315–325. [CrossRef]
157. Karami, K.; Abdolmaleki, A. Generalized second law of thermodynamics in $f(T)$ gravity. *J. Cosmol. Astropart. Phys.* **2012**, *2012*, 007. [CrossRef]

158. Lu, J.; Xu, L.; Li, J.; Chang, B.; Gui, Y.; Liu, H. Constraints on modified Chaplygin Gas from recent observations and a comparison of its status with other models. *Phys. Lett.* **2008**, *662*, 87–91. [CrossRef]
159. Karami, K. Chaplygin scalar field reconstruction of the modified ghost dark energy model. *Can. J. Phys.* **2015**, *93*, 855–861. [CrossRef]
160. Yang, H.; Wang, J. Concentration in vanishing pressure limit of solutions to the modified Chaplygin Gas equations. *J. Math. Phys.* **2016**, *57*, 111504. [CrossRef]
161. Saha, S.; Chattopadhyay, S. Viscous generalised Chaplygin Gas under the purview of $f(T)$ gravity and the model assessment through probabilistic information theory. *Phys. Scr.* **2022**, *97*, 045006. [CrossRef]
162. Chattopadhyay, S. A study on the bouncing behavior of modified Chaplygin Gas in presence of bulk viscosity and its consequences in the modified gravity framework. *Int. J. Geom. Methods Mod. Phys.* **2017**, *14*, 1750181. [CrossRef]